



Development of Silicon Sensor Technologies for the ATLAS Experiment Upgrades

and

Measurements of Heavy Quark Production Fractions with Fully Reconstructed D^{*+} Mesons with ATLAS

Jessica Metcalfe

April 25th, 2012

Argonne National Laboratory Interview Talk



Outline



- Introduction to the ATLAS Experiment
- Commissioning the Pixel Detector
- Upgrade Silicon R&D
 - Planar Technologies
 - 3D Sensors
 - SiGe HBT electronics
- Bottom and Charm Physics Data Analysis



Outline



- Introduction to ATLAS
- Commissioning the Pixel Detector
- Upgrade Silicon R&D
 - Planar Technologies
 - 3D Sensors
 - SiGe HBT electronics
- Bottom and Charm Physics Data Analysis



Introduction to ATLAS

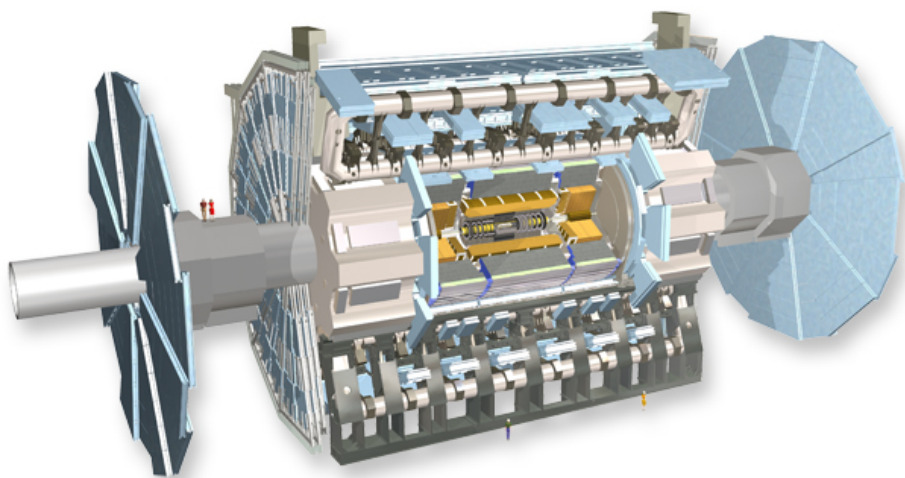


ATLAS Inner Detector:

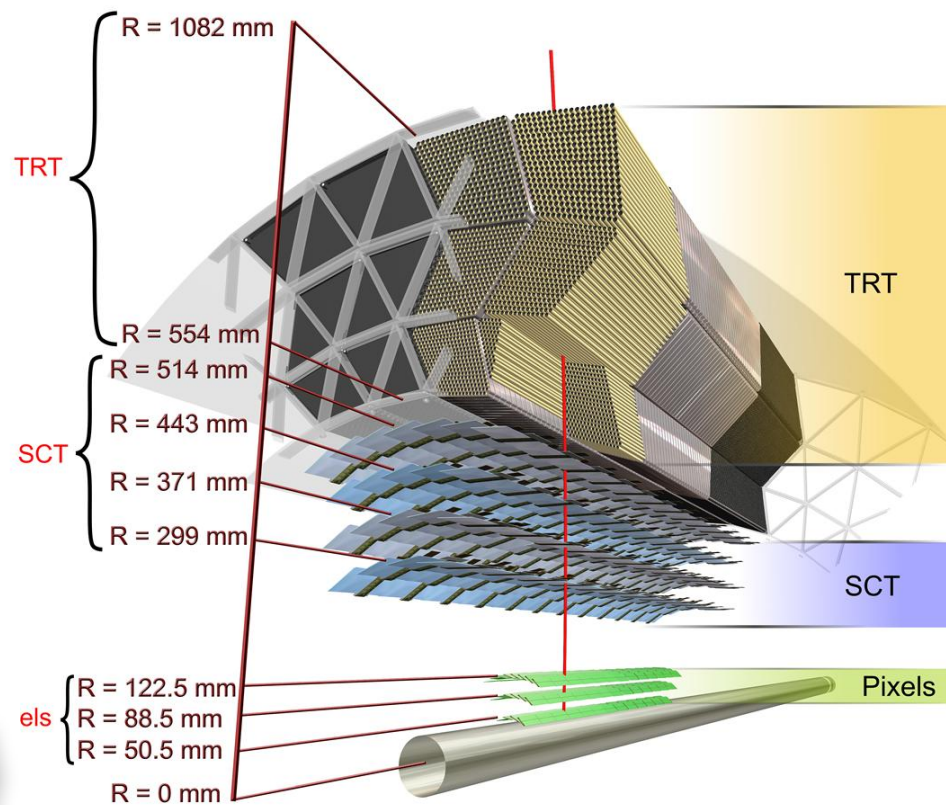
- tracks charged particles that traverse the detector

Silicon Detectors:

- Pixels
- SCT



April 25th, 2012



Silicon Detectors & b/c Physics
Jessica Metcalfe



Outline



- Introduction to ATLAS
- **Commissioning the Pixel Detector**
- Upgrade Silicon R&D
 - Planar Technologies
 - 3D Sensors
 - SiGe HBT electronics
- Bottom and Charm Physics Data Analysis

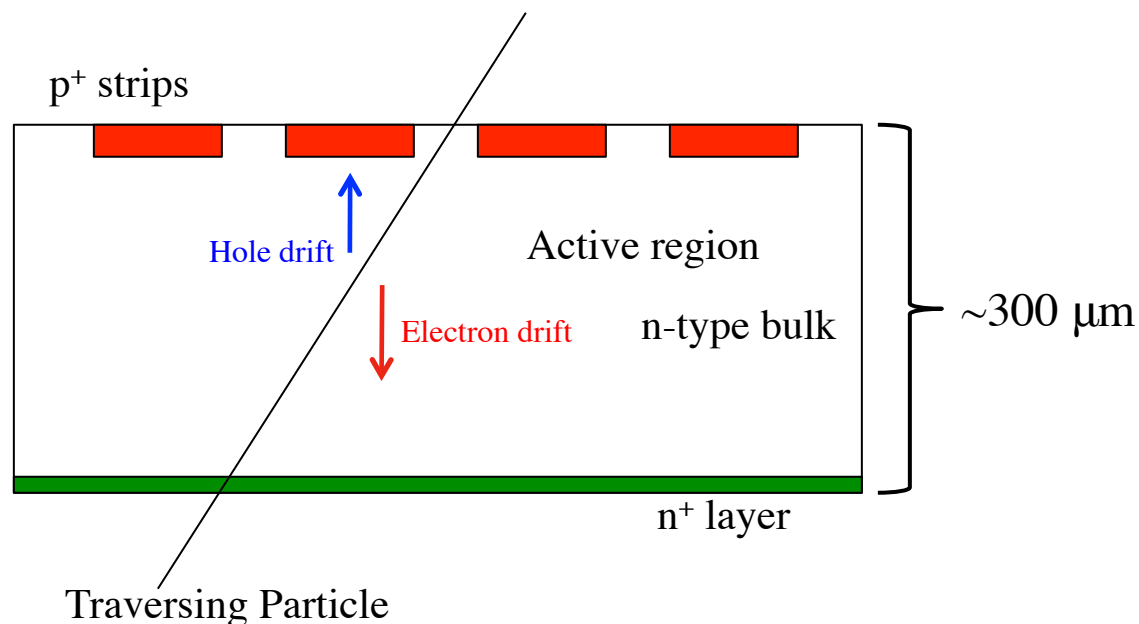


Silicon Sensor Background



Silicon Sensor

- Apply bias voltage (~ 100 - 500 V) to deplete the sensor
- MIP particle creates electron hole pairs
 - drift to strip implants and backplane
 - signal is read out by Front-End electronics



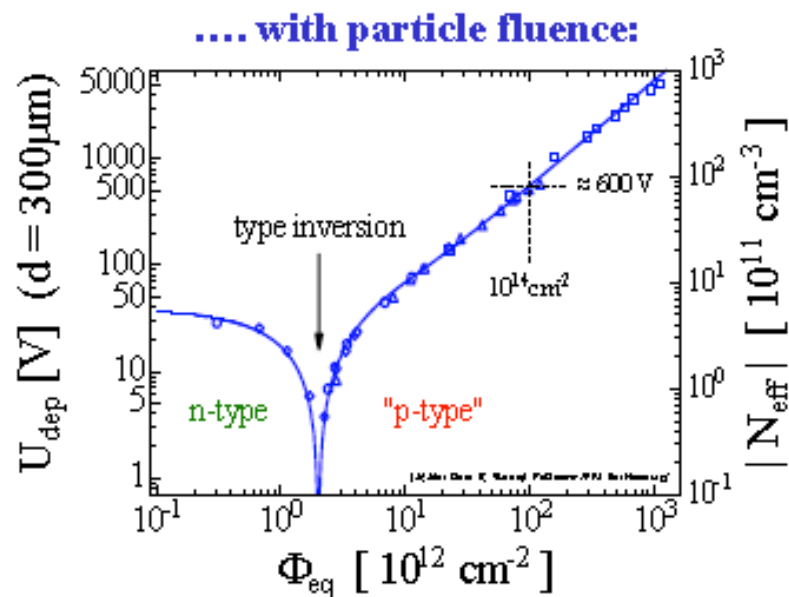


Silicon Sensor Background



ATLAS Pixel Sensor

- n-type silicon
- undergoes type inversion around $3 \times 10^{12} \text{ 1 MeV } n_{\text{eq}}/\text{cm}^2$
- requires more bias voltage to fully deplete the sensor



[M.Moll, PhD thesis 1992, University of Hamburg]



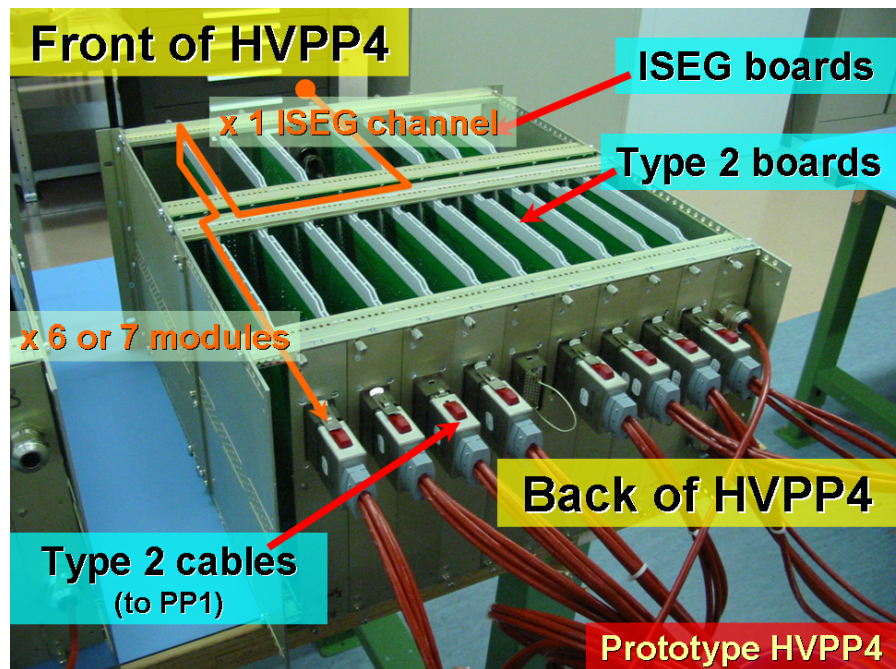
Commissioning



Pixel Detector: HVPP4

High Voltage Patch Panel 4—junction box to distribute the high voltage (bias voltage) to the pixel modules.

- modular design
 - accommodate changing power requirements over time
 - after type inversion, depletion voltage requirements increase
→ need ability to insert more power supplies
- prototype testing
- production module qualification
- radiation monitoring



Publication: HVPP4 Production Model Qualification Procedure: Jessica Metcalfe. CERN EDMS (Engineering & Equipment Data Management Service), ID 875443, October 2007.



Outline



- Introduction to ATLAS
- Commissioning the Pixel Detector
- Upgrade Silicon R&D
 - Planar Technologies
 - 3D Sensors
 - SiGe HBT electronics
- Bottom and Charm Physics Data Analysis

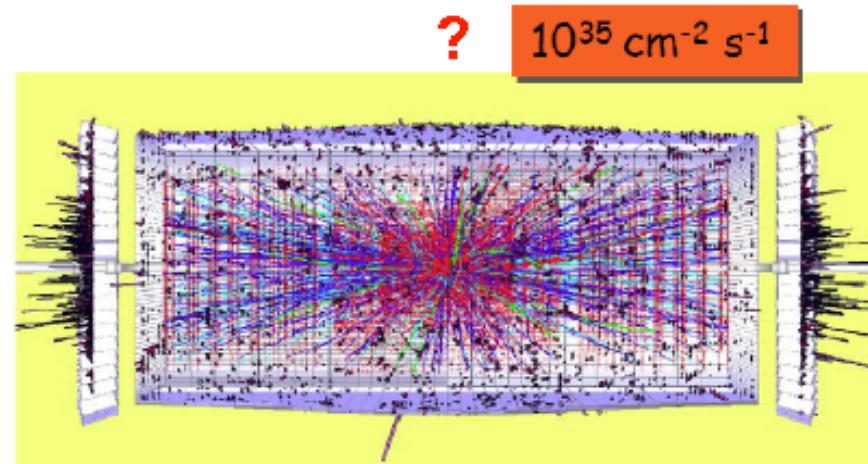
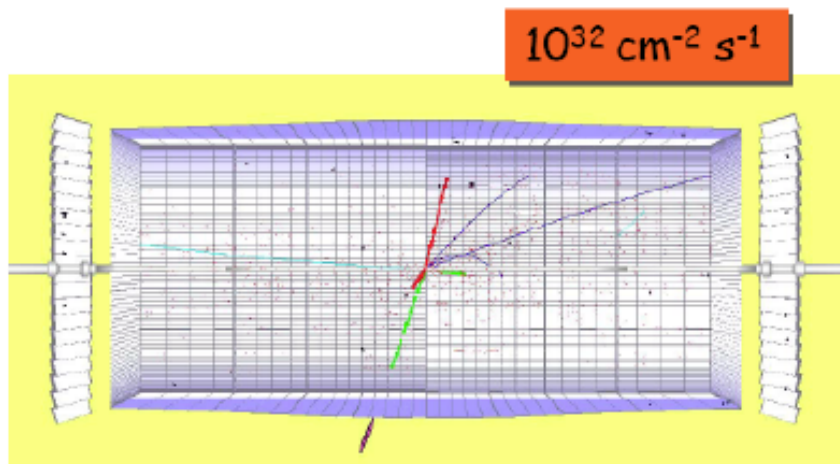


super-LHC



~2019 the LHC will be upgraded

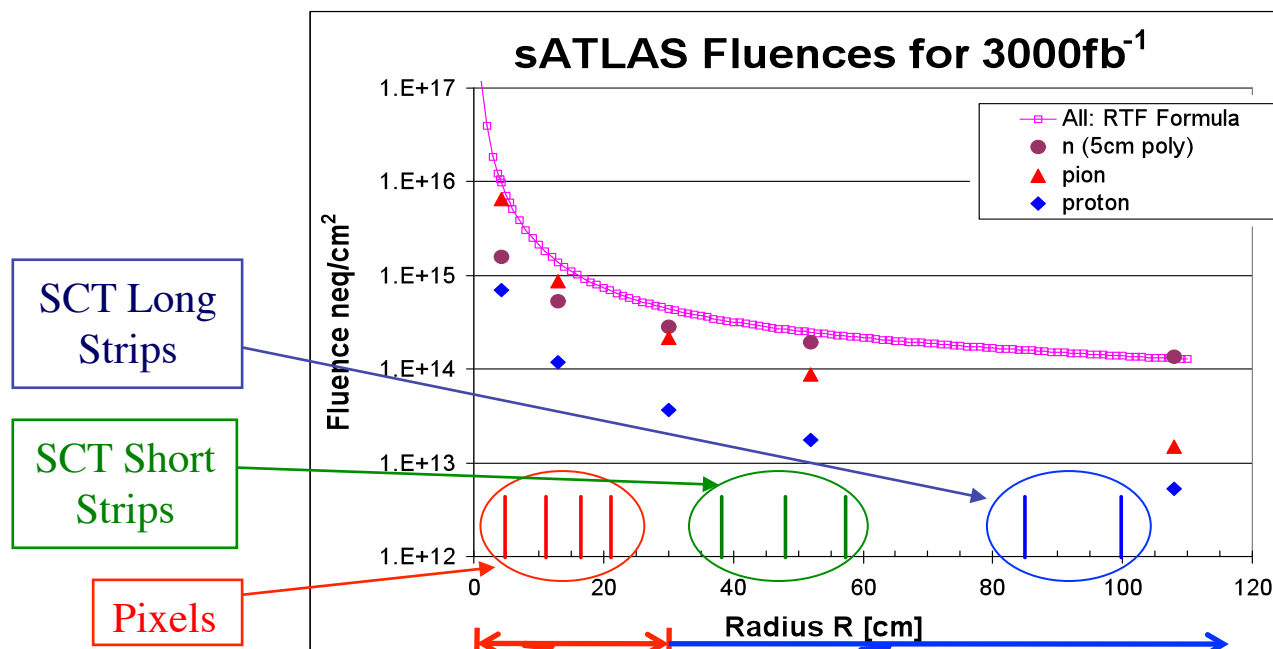
- luminosity increase from $1 \times 10^{33} \rightarrow 1 \times 10^{35} \text{ cm}^{-2} \cdot \text{s}^{-1}$



Michael Moll – Instrumentation Seminar, Hamburg 26.3.2010



ATLAS Upgrade



[ATLAS Radiation Taskforce [ATL-GEN-2005-01] & H. Sadrozinski [IEEE NSS 2007]]

Predicted fluences (n_{eq}), including safety factor 2:

- B layer ($r = 3.7$ cm) 2.5×10^{16} (1140 MRad)
- Inner pixel layer ($r = 5$ cm): 1.4×10^{16} (712 MRad)
- Second pixel layer ($r = 7$ cm): 7.8×10^{15} (420 MRad)
- Outer pixel layer ($r = 11$ cm): 3.6×10^{15} (207 Mrad)
- Short strips ($r = 38$ cm): 6.8×10^{14} (30 Mrad)
- Long strips ($r = 85$ cm): 3.2×10^{14} (8.4 Mrad)



Planar Silicon Sensors



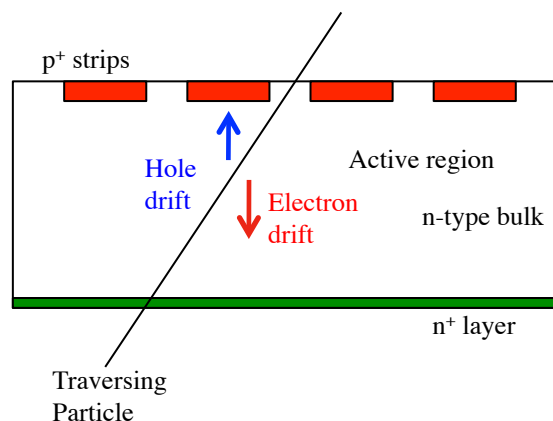
New types of planar Si sensors (candidates for Upgrade):

p-type silicon sensors: collect electrons instead of holes → yields lower trapping probability due to higher electron mobility

- no radiation-induced type inversion
- single-sided processing reduces cost

Czochralski silicon sensors: higher oxygen content → shown to require lower bias voltage for full depletion

- makes the formation of shallow Thermal Donors possible



Explore effects of particle irradiation:
proton, neutron, and gamma



Planar Sensors



Silicon sensor annealing:

- n- and p-type, Float Zone (Fz) and Magnetic Czochralski (MCz)
- underwent proton irradiation and annealing at 60 °C
 - Annealing: accelerates thermodynamic (diffusion) processes in the Si material
- measured:
 - leakage current vs bias voltage (IV)
 - capacitance vs bias voltage (CV)
- extracted: full depletion voltage (V_{fd}) and effective doping concentration (N_{eff})

	n-on-p Fz	p-on-n Fz	n-on-p MCz	p-on-n MCz
Manufacturer	HPK	Micron	Micron	Micron
Resistivity	13 k Ω -cm	3.3 k Ω -cm	1.9 k Ω -cm	1.4 k Ω -cm
Active Area	3mm \times 3mm	3mm \times 3mm	3mm \times 3mm	3mm \times 3mm
Thickness	300 μ m	300 μ m	300 μ m	300 μ m
Initial V_{fd}	75 V	95 V	520 V	220 V
$N_{eff,0}$	$-1.1 \times 10^{12} \text{ cm}^{-3}$	$1.39 \times 10^{12} \text{ cm}^{-3}$	$-7.59 \times 10^{12} \text{ cm}^{-3}$	$3.21 \times 10^{12} \text{ cm}^{-3}$



Planar Sensors

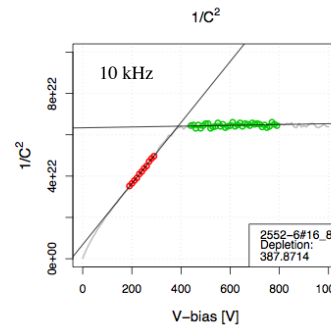


Characteristic Measurements:

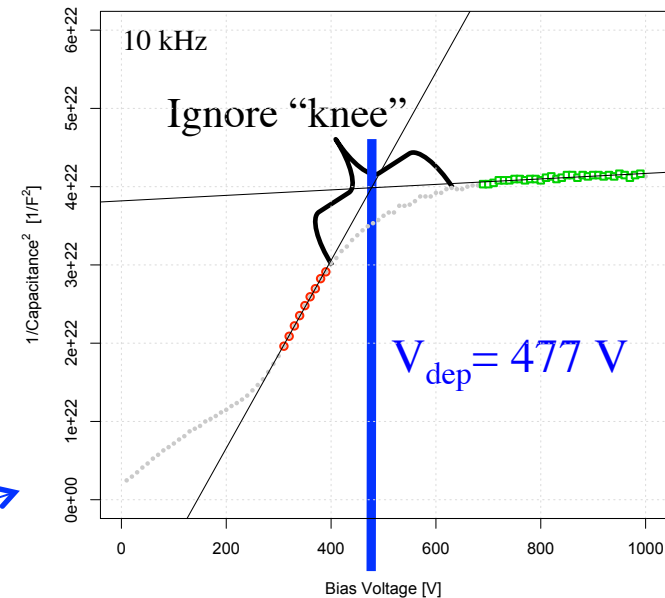
- *Depletion Voltage*
- *Effective Doping Concentration*
- Leakage Current

Method for Depletion Voltage:

- leakage current, I_V
 - check for nominal operation (i.e. no thermal runaway)
- measure capacitance in good region
- extract full depletion voltage



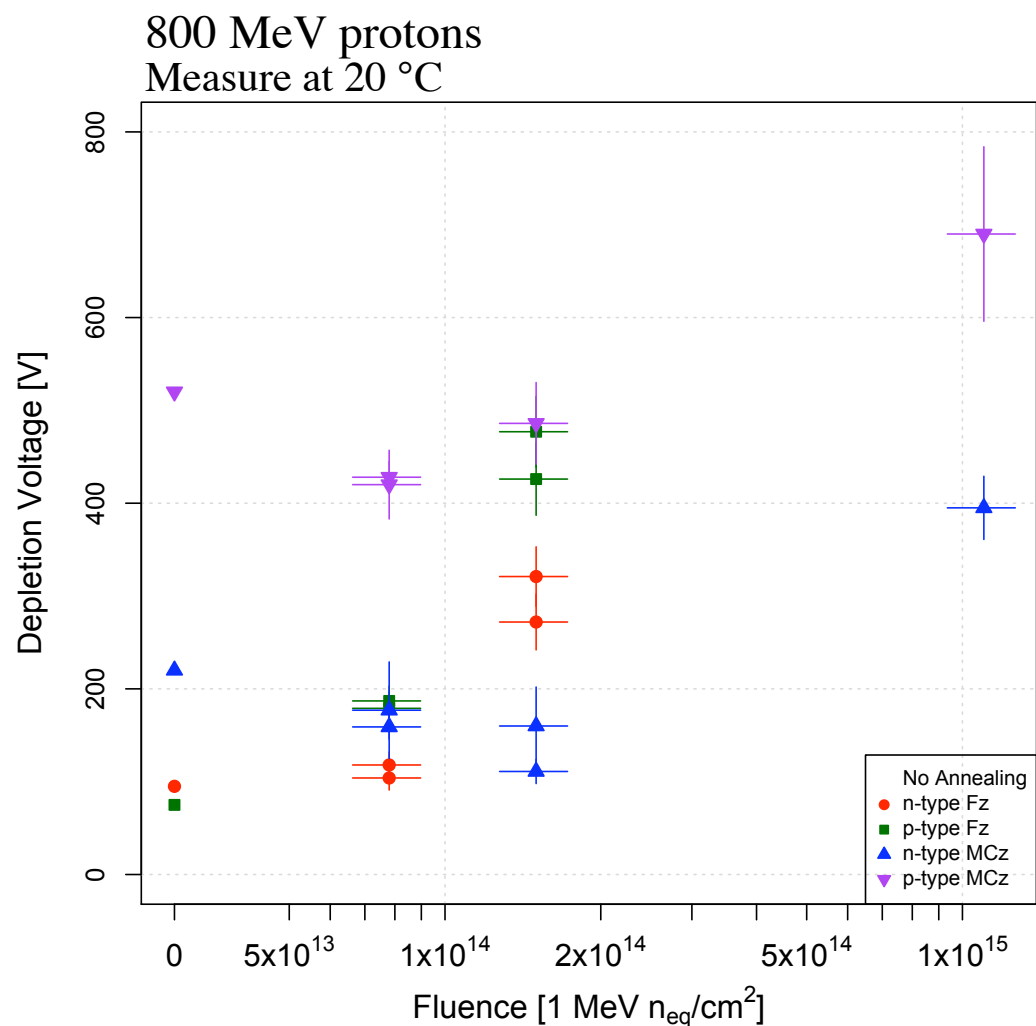
n-on-p MCz irradiated to $7.8 \times 10^{13} \text{ n}_{\text{eq}}/\text{cm}^2$ after 80 minutes anneal time at 60°C .



n-on-p MCz irradiated to $1.1 \times 10^{15} \text{ n}_{\text{eq}}/\text{cm}^2$ after 80 minutes anneal time at 60°C .



Planar Sensors



- Compared *n-* and *p-*type Float Zone (Fz) and MCz materials
- irradiated with 800 MeV protons

Fluence Dependence:

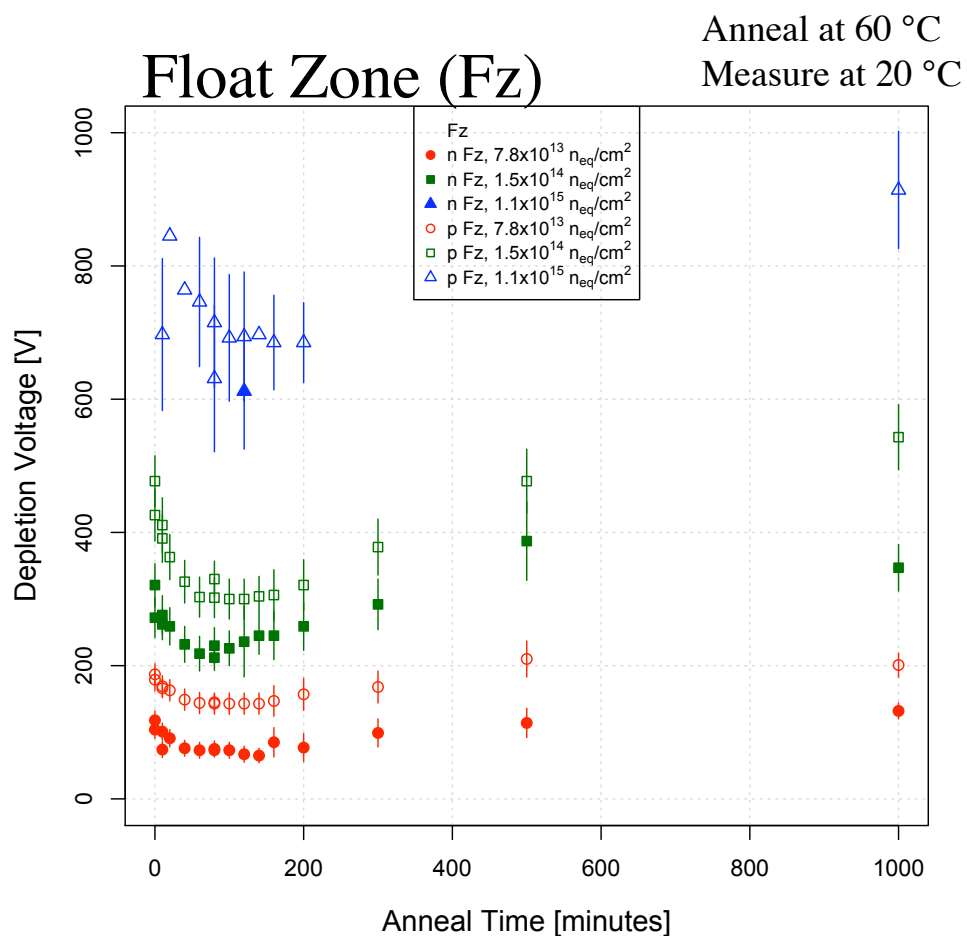
- Fz diodes start with lower depletion voltage, but break down before full depletion at highest fluence
- MCz diodes improve with low fluence and show gradual increase in depletion voltage at higher fluences



Planar Sensors



800 MeV protons



Fz Diodes:

- depletion voltage decreases for ~100 minutes then increases
- proton irradiations introduce positive space charge (sc)
- two main annealing processes (independent of device type):
 - short-term: decrease of acceptor-like defects, increases sc
 - long-term: acceptors are activated, decreases sc
- changes in V_{fd} is amplified for higher fluences

Device:

	n-type Fz	p-type Fz
Before Irradiation	+sc	-sc
After Irradiation	-sc	-sc



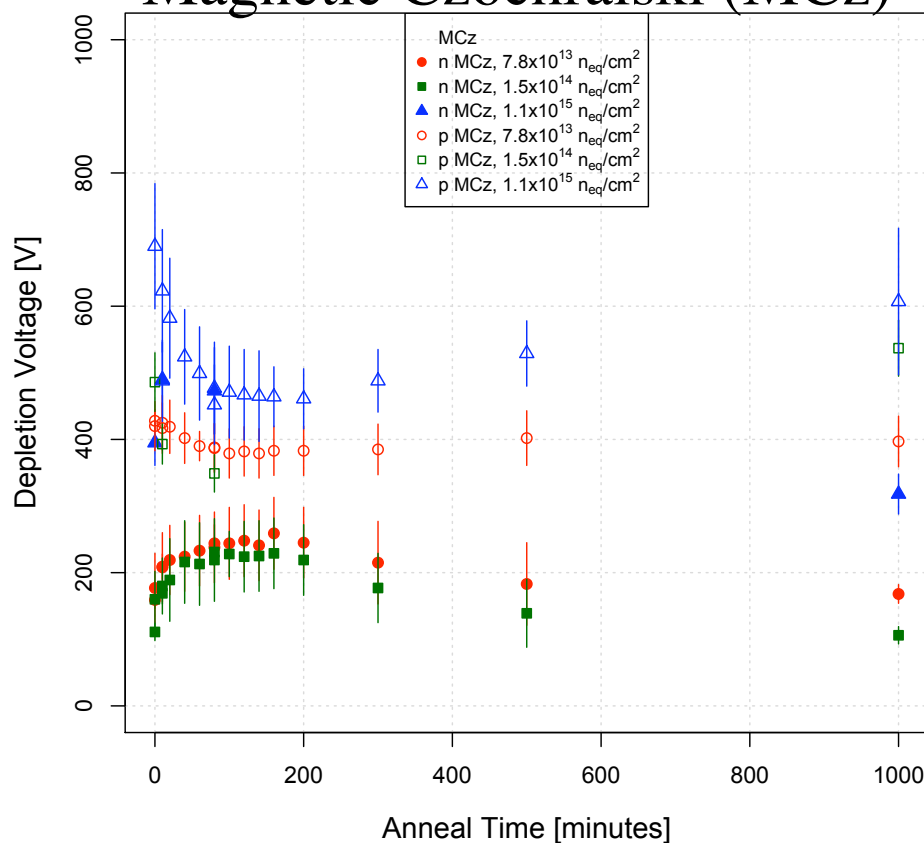
Planar Sensors



800 MeV protons

Anneal at 60 °C
Measure at 20 °C

Magnetic Czochralski (MCz)



MCz Diodes:

- depletion voltage decreases/increases for ~100 minutes then increases/decreases
- n-type has opposite change in V_{fd} due to space charge (sc)
 - short-term: increases sc
 - long-term: decreases sc

Device:		
	n-type MCz	p-type MCz
Before Irradiation	+sc	-sc
After Irradiation	+sc	-sc



Planar Sensors

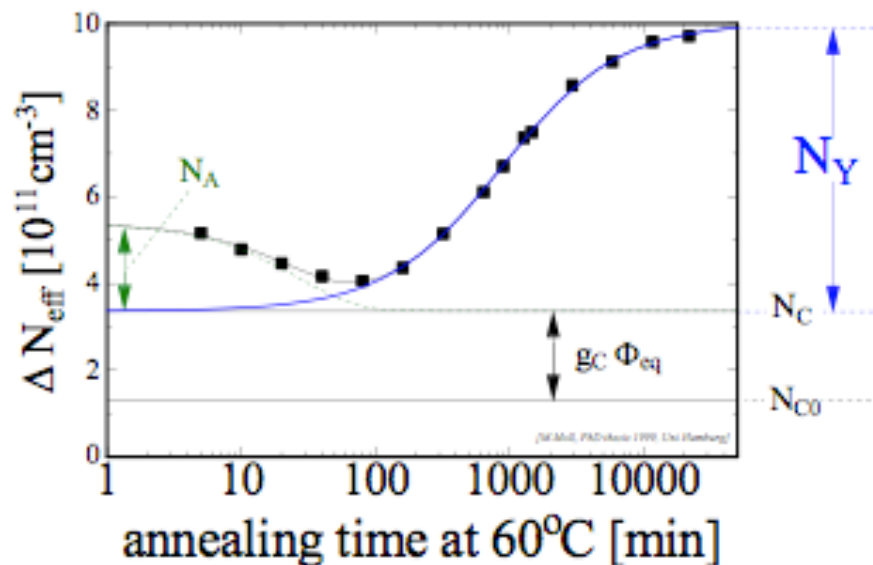


Convert V_{fd} to the effective doping concentration, N_{eff} , in order to apply the Hamburg Model for annealing:

$$|N_{eff}| = V_{fd} \frac{2\epsilon_{Si}}{ed^2}$$

- The sign of the N_{eff} was inferred from the space charge determined from the previous results

Hamburg Model



$$\Delta N_{eff} = N_A(\Phi, t) + N_C(\Phi) + N_Y(\Phi, t)$$

$$N_A(\Phi, t) = g_a e^{-t/\tau_a} \Phi \quad (\text{short term annealing})$$

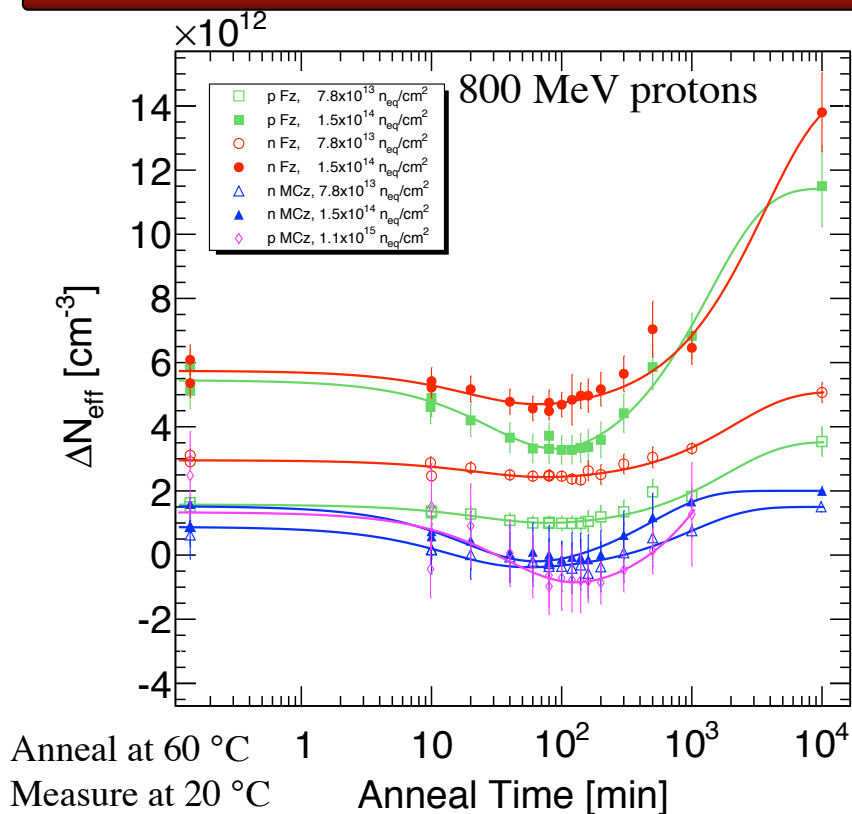
$$N_C(\Phi) = g_c \Phi + N_{c0}(1 - e^{-c\Phi}) \quad (\text{stable damage})$$

$$N_Y(\Phi, t) = g_Y(1 - e^{-t/\tau_Y}) \Phi \quad (\text{long term annealing})$$

[4] M. Moll, Thesis Uni. Hamburg, DESY-THESIS-1999-040



Planar Sensors



Observations:

- The time constants describing the short and long-term annealing are well separated
- Hamburg Model describes the physical processes well
 - short term: decrease of acceptor-like defects
 - long-term: acceptors are activated
- independent of the type of device
- introduction rates g_a and g_Y are consistent within device type

	g_a [cm^{-1}]	g_Y [cm^{-1}]	N_c [cm^{-3}]	τ_a [min]	τ_Y [min]
n-on-p Fz $7.8e13$	0.02 ± 0.02	0.04 ± 0.03	$2 \times 10^{11} \pm 2 \times 10^{12}$	32 ± 22	1700 ± 800
n-on-p Fz $1.5e14$	0.02 ± 0.004	0.058 ± 0.009	$2.5 \times 10^{12} \pm 6 \times 10^{11}$	36 ± 19	1300 ± 500
p-on-n Fz $7.8e13$	0.009 ± 0.003	0.035 ± 0.005	$2.3 \times 10^{12} \pm 2 \times 10^{11}$	27 ± 26	2000 ± 700
p-on-n Fz $1.5e14$	0.01 ± 0.007	0.06 ± 0.02	$-1.10 \times 10^{13} \pm 1 \times 10^{12}$	24 ± 17	3400 ± 1400
n-on-p MCz $1.1e15$	0.003 ± 0.001	-	-	-	-
p-on-n MCz $7.8e13$	0.018 ± 0.005	0.03 ± 0.02	$-5 \times 10^{11} \pm 4 \times 10^{11}$	17 ± 16	1100 ± 1600
p-on-n MCz $1.5e14$	0.014 ± 0.003	0.018 ± 0.003	$-6 \times 10^{11} \pm 4 \times 10^{11}$	22 ± 13	500 ± 200



Planar Sensors



Summary of Annealing Study:

- Direct comparison of suite of devices
 - n- and p-type, Fz and MCz
- Beneficial annealing (decrease in V_{fd}) observed during first ~ 100 minutes for devices with -sc after proton irradiation
 - n-Fz, p-Fz, p-MCz
- Initial increase in V_{fd} during first ~ 100 minutes for n-type MCz with +sc after proton irradiation
- The introduction rates and time constant parameters were extracted using the Hamburg Model on a suite of n- and p-type Fz and MCz diodes for the first time.
 - introduction rates are consistent for each device type
 - excellent consistency for short term annealing time constant and separation from long-term annealing time constants
 - the results support the claim that the same physical process occurred in all the devices as described by the Hamburg Model
- Understanding the underlying processes contributing to the annealing behavior of silicon detectors is key to predict the performance during periods where detectors are not kept at below freezing temperatures

Publication: *Annealing Effects on Depletion Voltage and Capacitance of Float Zone and Magnetic Czochralski Silicon Diodes After 800 MeV Proton Exposure*: **J. Metcalfe**, M. Hoferkamp, S. Seidel. IEEE NSS/MIC Conference Record N21-5 November 2010.

Talks: 2010 IEEE Nuclear Science Symposium, Knoxville, Tennessee, USA

June 2009 RD50 Workshop, Freiburg, Germany

April 25th, 2012

Silicon Detectors & b/c Physics
Jessica Metcalfe

20



Outline



- Introduction to ATLAS
- Commissioning the Pixel Detector
- Upgrade Silicon R&D
 - Planar Technologies
 - 3D Sensors
 - SiGe HBT electronics
- Bottom and Charm Physics Data Analysis



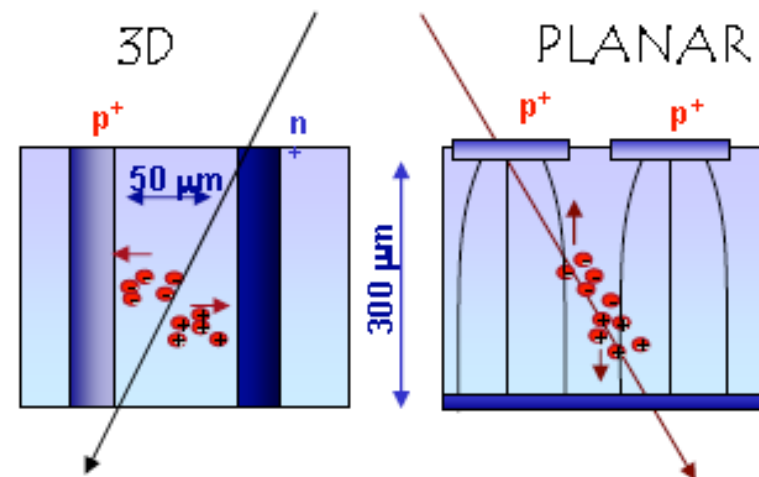
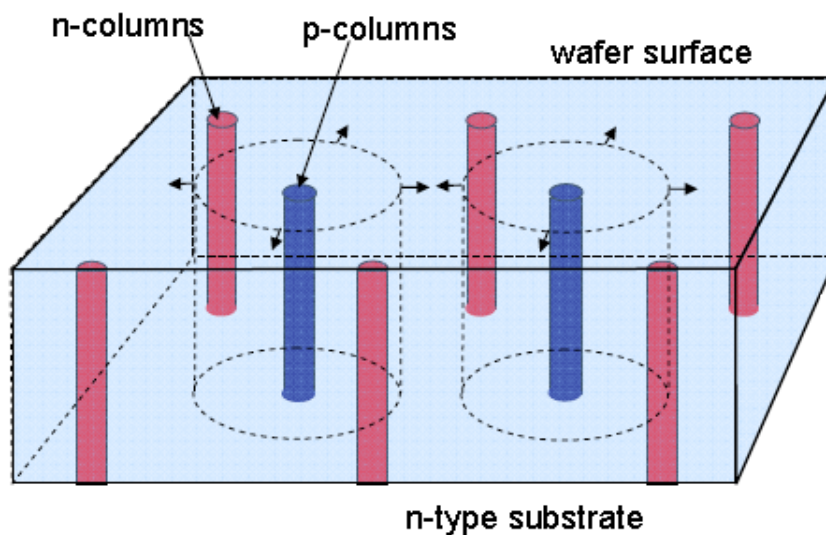
3D Silicon Sensors



3D electrodes:

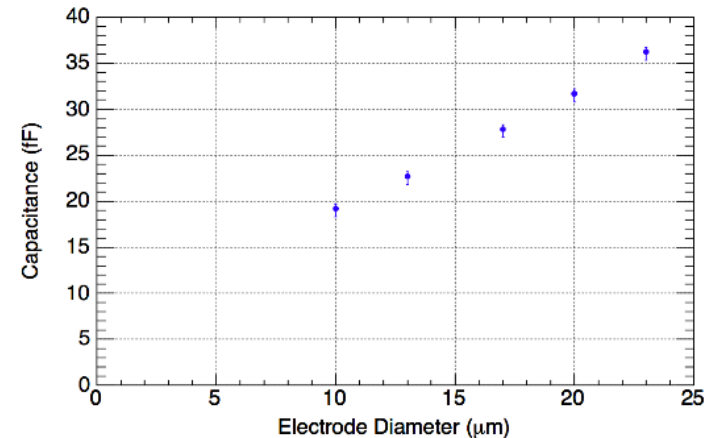
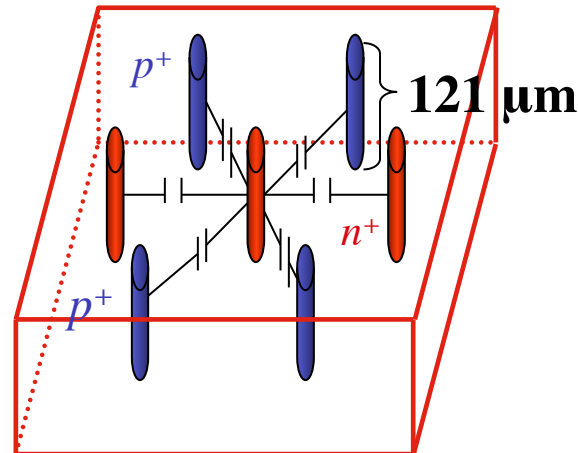
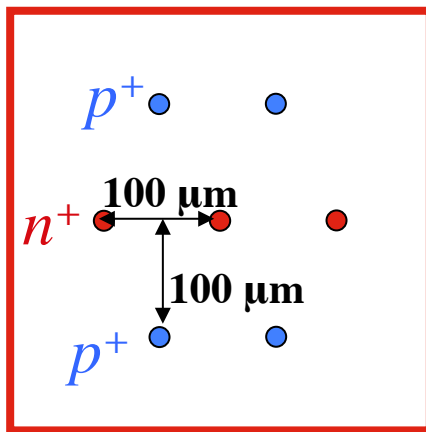
narrow columns along detector thickness

- depletion occurs laterally
- decouples detector thickness from charge collection
- reduced distance between electrodes
 - lower depletion voltage needed
 - fast signal
- radiation hard





3D Sensors



Capacitance Simulation and Measurement

- Devices:
100 μm electrode spacing, 17 μm electrode diameter, 121 μm length
- irradiated by 55 MeV protons
- no annealing
- pre-irradiation simulation
- direct and indirect measurements

April 25th, 2012

Silicon Detectors & b/c Physics
Jessica Metcalfe

Simulation:

- Capacitance was predicted from a geometrical model using an electrostatic simulation--IES Coulomb
- An electrode and its 6 nearest neighbors were simulated in Si bulk material with a substrate layer.
- The capacitance was 28 fF at 17 μm .

23



3D Sensors

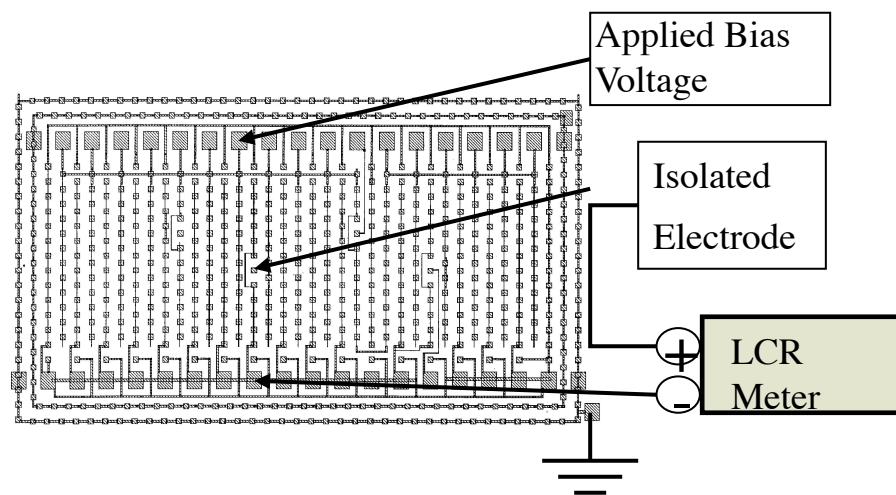
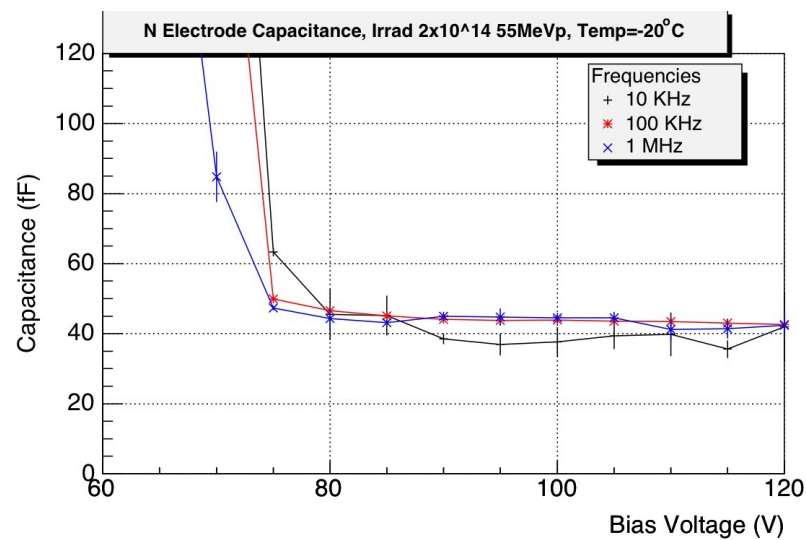


Image from S. Parker and C. Kenney, IEEE Trans. Nucl. Sci., Vol. 48 p. 1629, 2001.

Direct Capacitance Measurement



- Measure isolated electrode capacitance while bias voltage is applied
- Measurements performed at $-20\text{ }^{\circ}\text{C}$ to suppress leakage current
- Capacitance was determined from the average capacitance for each frequency above depletion voltage



3D Sensors



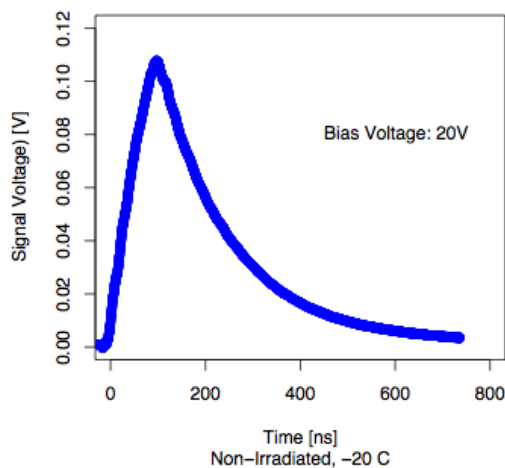
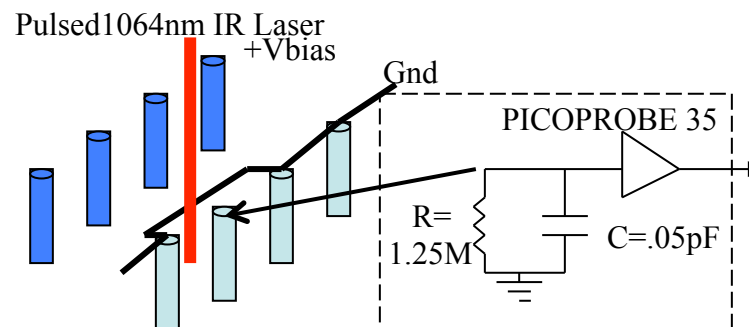
Indirect Capacitance Measurement

- laser pulse stimulates current
- decay constant extracted:

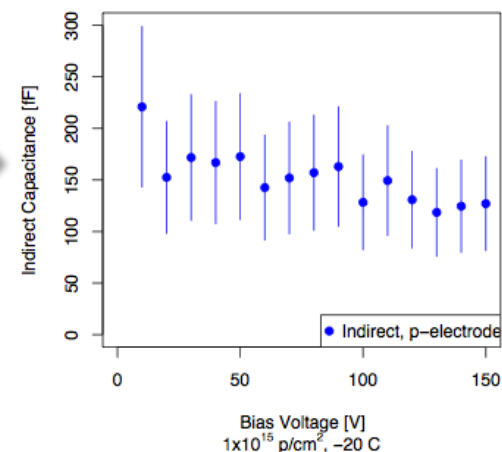
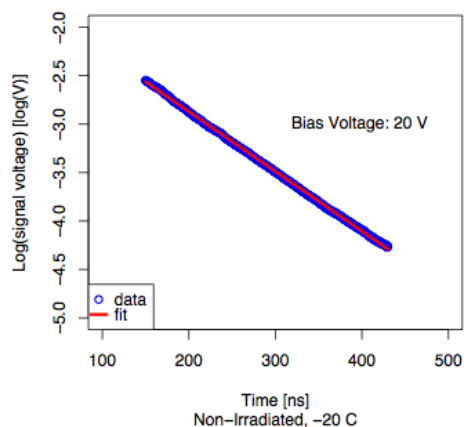
$$V = V_0 e^{-t/\tau}$$

where $\tau = R_{\text{probe}} (C_{\text{probe}} + C_{3D})$

and $R_{\text{probe}} = 1.25\text{M}\Omega$ and $C_{\text{probe}} = 0.05\text{pF}$



$$V = V_0 e^{-t/\tau}$$



April 25th, 2012

Silicon Detectors & b/c Physics
Jessica Metcalfe

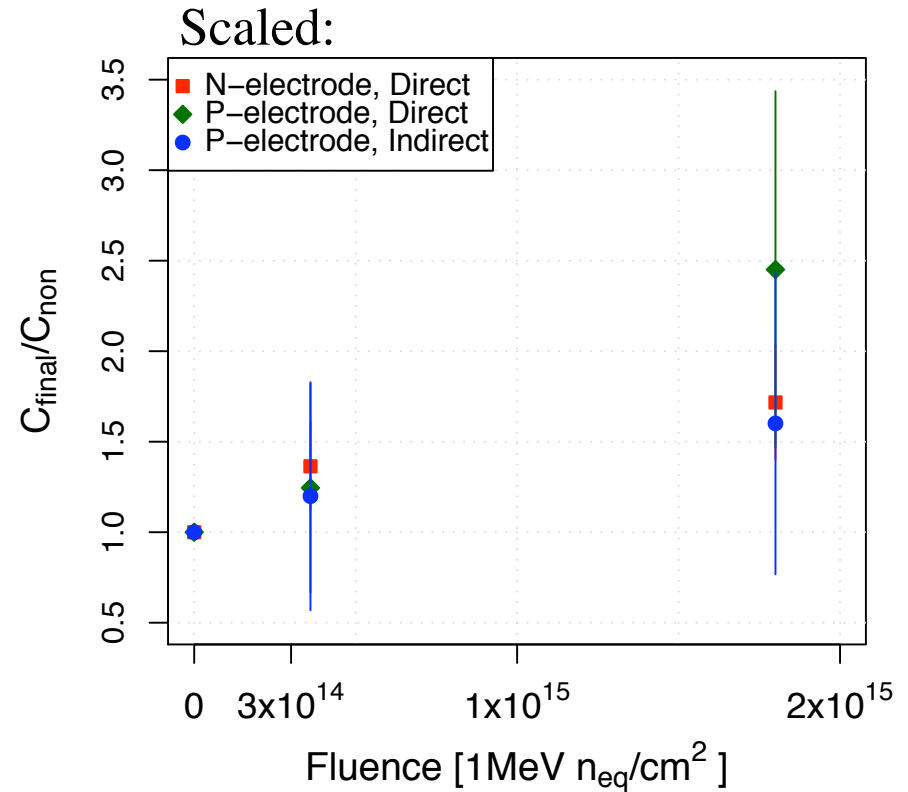
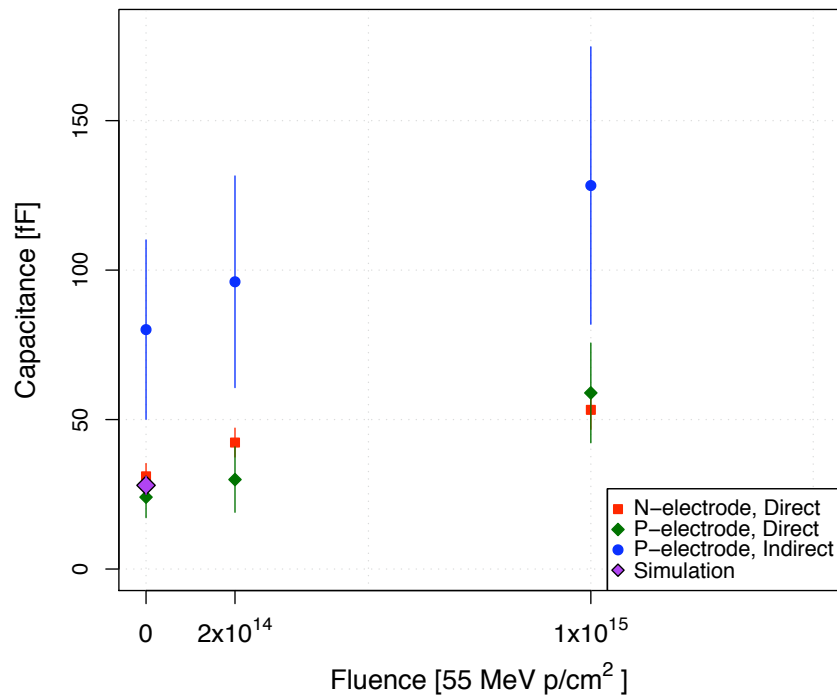
25



3D Sensors



Results:



- Capacitance depends on fluence
- Measurement methods agree—better at lower fluences



3D Sensors



Summary of 3D Sensor Study:

- Measure capacitance of irradiated 3D sensors for the first time
- Compared 3D simulation to direct and indirect capacitance measurement techniques
- Inter-electrode capacitance was found to increase with proton fluence
 - by 70% from non-irradiated to 1×10^{15} p/cm² (55 MeV protons)
- Capacitance effects the noise in the detector as well as the read-out electronics design

Publication: Capacitance Simulations and Measurements of 3D Pixel Sensors Under 55 MeV Proton Exposure: J. Metcalfe, I. Gorelov, M. Hoferkamp, S. Seidel. IEEE Transactions on Nuclear Science, Vol 55, Issue 5, pp2679-2684, October 2008.

Talk: 2007 IEEE Nuclear Science Symposium, Honolulu, Hawaii, USA



Outline



- Introduction to ATLAS
- Commissioning the Pixel Detector
- Upgrade Silicon R&D
 - Planar Technologies
 - 3D Sensors
 - SiGe HBT electronics
- Bottom and Charm Physics Data Analysis

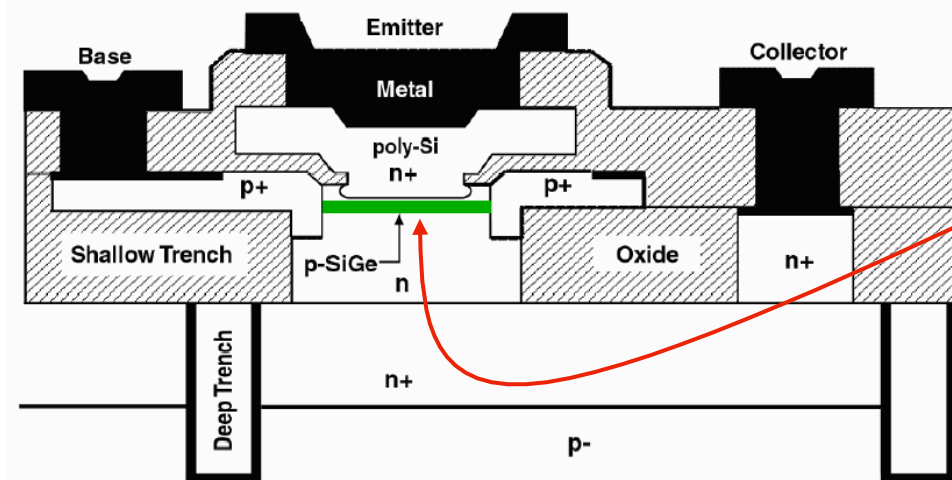


SiGe HBTs



Silicon Germanium (SiGe) Heterojunction Bipolar Transistors (HBTs)

- smaller bias current than CMOS designs
- low base resistance (10-100 Ω) translates to very low noise at low bias currents
- fast shaping time (order of tens of nanoseconds to distinguish particle beam bunches)
- can handle large capacitive loads (ex: 5-15 pF for Si strips)



Origin of radiation tolerance:

- Small active volume of the transistor
- Thin emitter-base spacer oxide (weakest spot)



SiGe HBTs

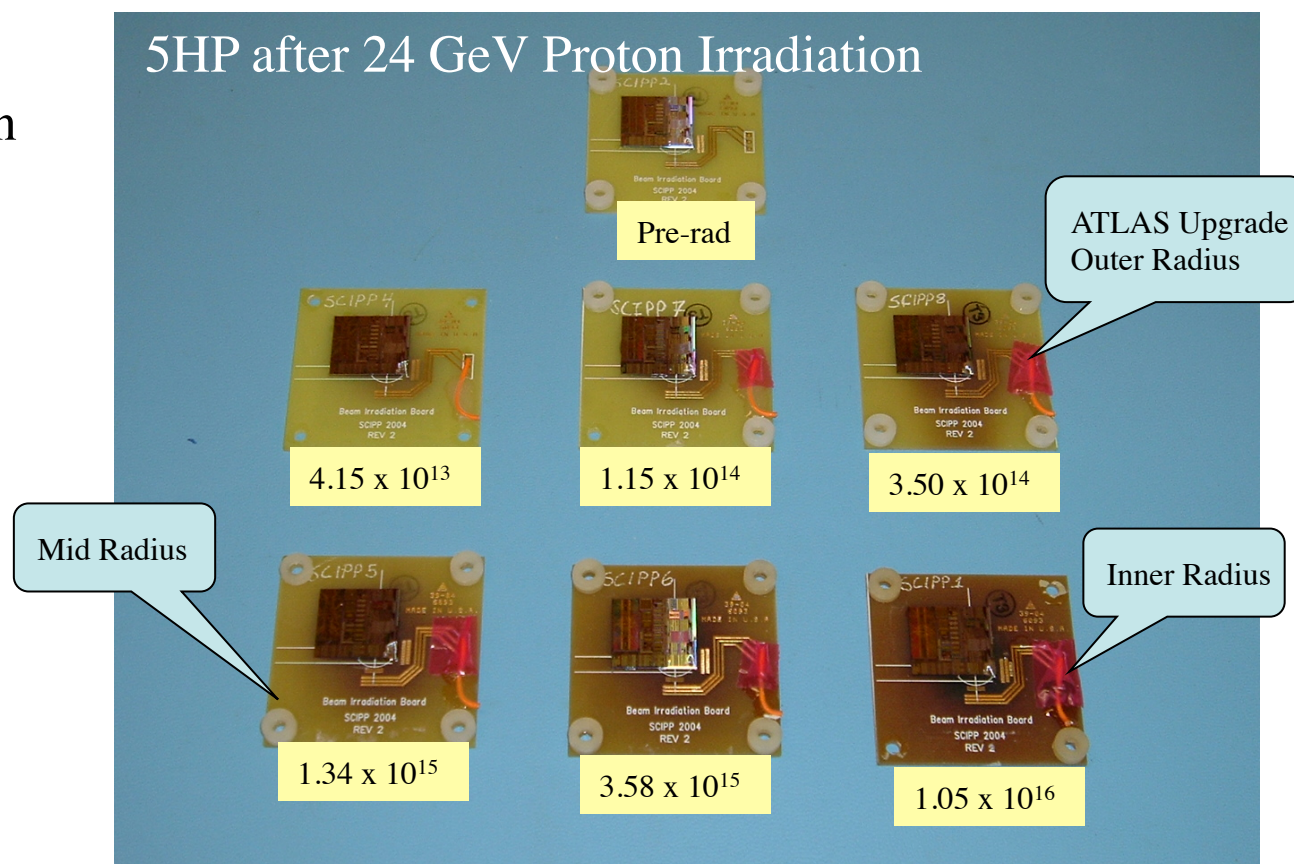


- Investigated IBM 5HP, 7HP, 8HP technologies after proton, neutron and gamma irradiation

- Measured current gain
- performed annealing studies

Type:	size (μm^2)
5AM HBT:	0.5x1
	0.5x2.5
	0.5x20
7HP HBT:	0.2x2.5
	0.2x5
	0.28x5
8HP HBT:	0.12x2
	0.12x4
	0.12x8

5HP after 24 GeV Proton Irradiation



April 25th, 2012

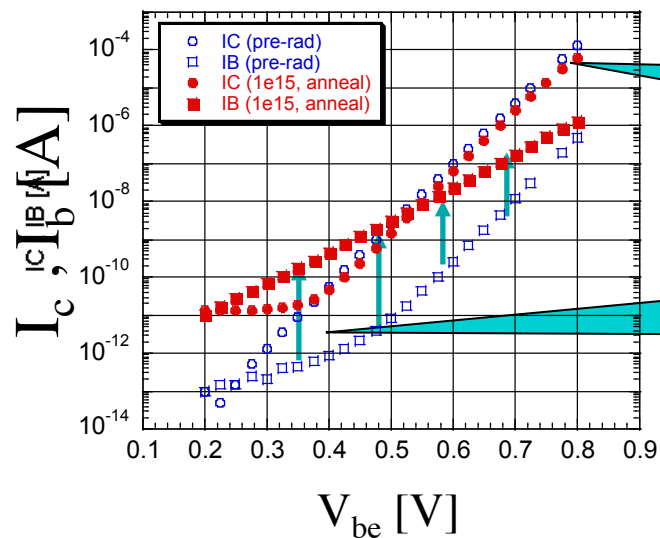


Forward Gummel Plot for $0.5 \times 2.5 \mu\text{m}^2$

I_c, I_b vs. V_{be} Pre-rad and After $1 \times 10^{15} \text{ p/cm}^2$ & Anneal Steps

Radiation damage increases base current causing the gain of the device to degrade.

Gain = I_c / I_b (collector current/base current)



Collector current remains the same

Base current increases after irradiation

Ionization Damage (in the spacer oxide layers)

- The charged nature of the particle creates oxide trapped charges and interface states in the emitter-base spacer increasing the base current.

Displacement Damage (in the oxide and bulk)

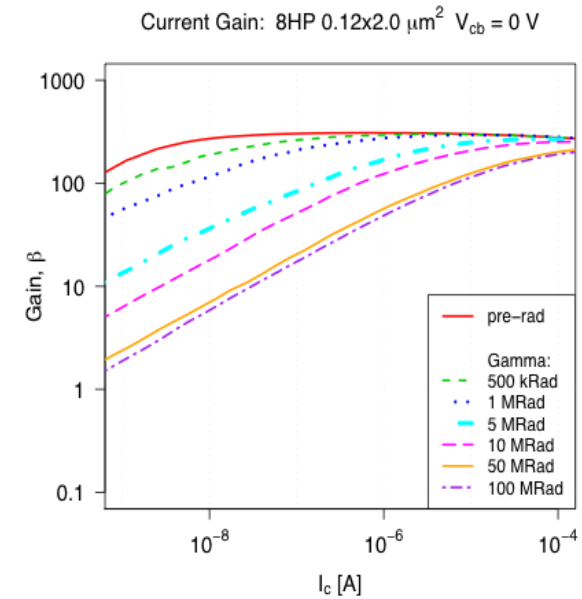
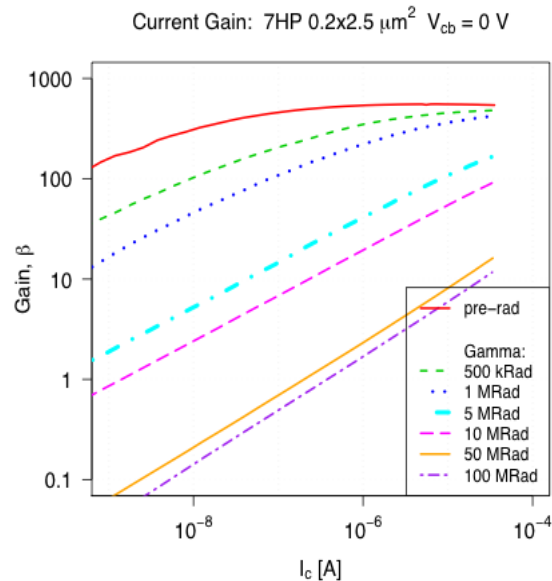
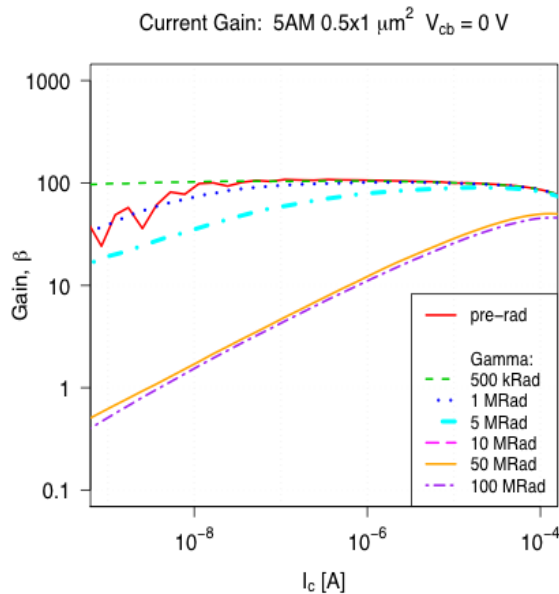
- The incident mass of the particle knocks out atoms in the lattice structure shortening hole lifetime, which is inversely proportional to the base current.



SiGe HBTs



5AM vs 7HP vs 8HP:



The 8HP performs best overall. The damage mechanism in the 7HP is distinctly different due to structural differences.

“ Ionizing radiation has been shown to damage the EB spacer region in these SiGe HBTs, and produce a perimeter-dependent space-charge generation/recombination (G/R) base-current leakage component that progressively degrades the base current (and current gain) as the fluence increases. ...the 7HP device degrades much more rapidly than the 5HP device. This result is consistent with significantly higher EB electric field under the EB spacer region in the 7HP device, which has both more abrupt doping profiles...as well as a decreased EB spacer thickness compared to the 5HP device...”

Silicon-Germanium Heterojunction Bipolar Transistors,

Cressler, Niu

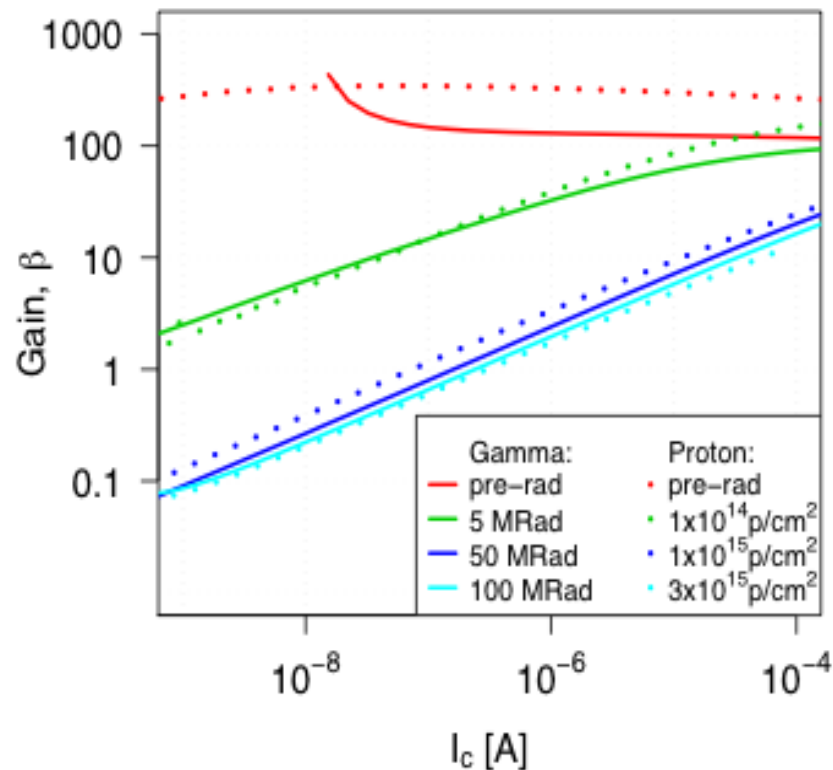


SiGe HBTs



Gamma vs Proton Damage:

Current Gain: 5AM 0.5x20 μm^2



The damage caused by gammas and protons for comparable doses/fluences is very similar even though starting gain values are different. This implies that most of the gain degradation is induced by ionization damage.



SiGe HBTs



Design Qualification:

Qualifications for a good transistor:

A gain of 50 is a good figure of merit for a transistor to use in a front-end circuit design.

Requires only 0.28 μA to reach a gain of 50!!

$\beta=50$
100 MRad

Type:	size (μm^2)	I_C (μA)	J_C ($\mu\text{A}/\mu\text{m}^2$)
5AM HBT Shorted:	0.5x1	145	290
	0.5x2.5	216	173
	0.5x20	179	18
7HP HBT Shorted:	0.2x2.5	217	434
	0.2x5	62	62
	0.28x5	83	30
8HP HBT Shorted:	0.12x2	1.0	4.2
	0.12x4	2.0	4.2
	0.12x8	3.8	3.9
8HP HBT Biased:	0.12x4	0.28	0.58

At 100 Mrad (before annealing), the dose reached at the mid-region of ATLAS Upgrade, very small currents can be used in the design of the front transistor and the others in a Front-End Channel design. This provides flexibility in choosing the operating current for the transistor, which allows the FEC design to optimize other factors such as matching.



SiGe HBTs



Summary:

- damage mainly due to ionization damage in oxide regions
 - comparable gamma and proton irradiation results
- power consumption still lower than CMOS
- acceptable gain after irradiation for several applications
- causes increase in the base current while collector current is stable
 - decreases current gain
- found acceptable gain after irradiation for several applications

Publications: Evaluation of the Radiation Tolerance of SiGe Heterojunction Bipolar Transistors Under 24-GeV Proton Exposure: J. Metcalfe, D.E. Dorfan, A. A. Grillo, A. Jones, D. Lucia, F. Martinez-McKinney, M. Mendoza, M. Rogers, H. F. -W. Sadrozinski, A. Seiden, E. Spencer, M. Wilder, J. D. Cressler, G. Prakash, A. Sutton. IEEE Transactions on Nuclear Science, Vol 53, Issue 6, pp 3889-3893, December 2006.

Evaluation of the Radiation Tolerance of Several Generations of SiGe Heterojunction Bipolar Transistors Under Radiation Exposure: Jessica Metcalfe, D.E. Dorfan, A.A. Grillo, A. Jones, F. Martinez-McKinney, P. Mekhedjian, M. Mendoza, H.F.-W. Sadrozinski, G. Saffier-Ewing, A. Seiden, E. Spencer, M. Wilder, R. Hackenburg, J. Kierstead, S. Rescia, J.D. Cressler, G. Prakash and A. Sutton; Nuclear Instruments and Methods A, Vol 579, Issue 2, pp 833-838, September 2007.

Talks: 2005 IEEE Nuclear Science Symposium, Puerto Rico, USA

June 2006 RD50 Workshop, Prague, Czech Republic

April 25th, 2012

Silicon Detectors & b/c Physics

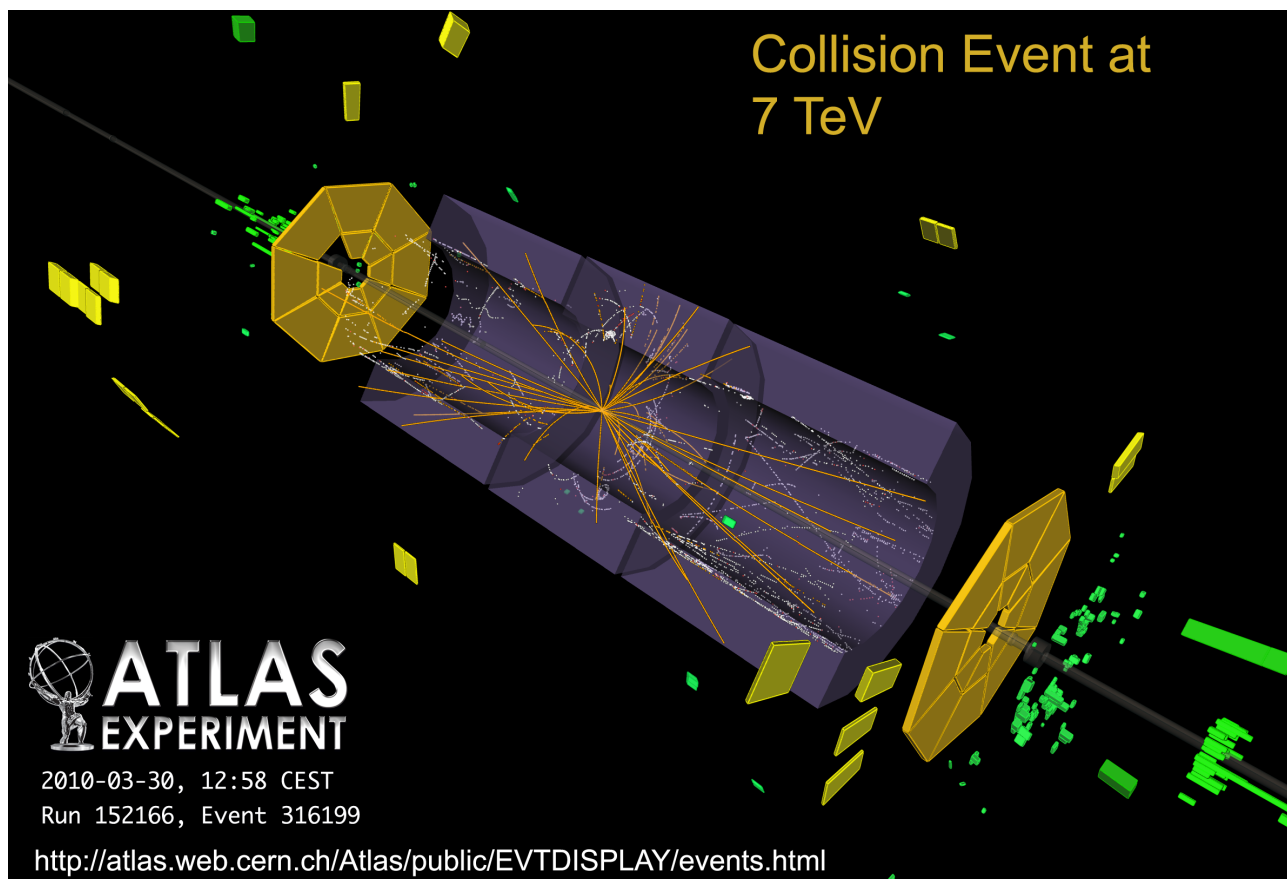
Jessica Metcalfe



Outline



- Introduction to ATLAS
- Commissioning the Pixel Detector
- Upgrade Silicon R&D
 - Planar Technologies
 - 3D Sensors
 - SiGe HBT electronics
- Bottom and Charm Physics Data Analysis



Data taking:

- Early 7 TeV physics event
- Tracking, MinBias scintillators, calo cells, muon detectors

April 25th, 2012

Silicon Detectors & b/c Physics
Jessica Metcalfe

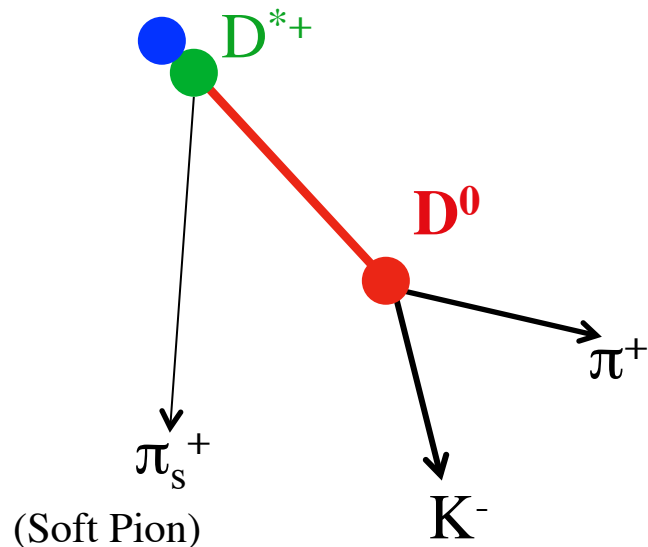


The Event



$D^{*+} \rightarrow D^0 \pi_s^+$, where $D^0 \rightarrow K^- \pi^+$ (+ c.c.)

c or b particle?

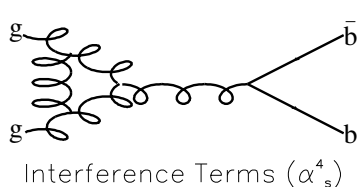
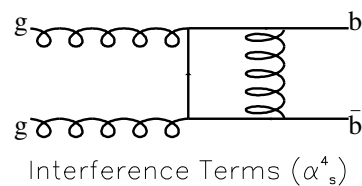
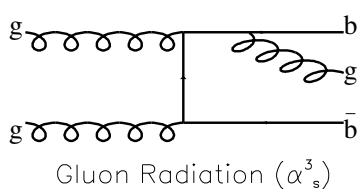
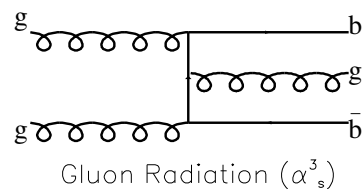
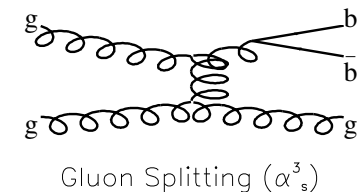
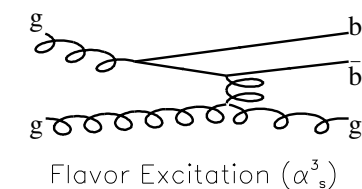
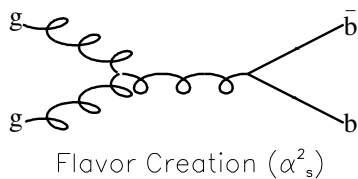
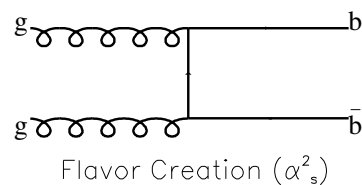


Measurement:

- What flavor is the D^{*+} 's parent?
 - produced via charm production at the primary vertex (produced promptly)
 - decay product of a B meson away from the primary vertex



Motivation



Motivation :

- heavy flavor events are background processes for new physics like $H \rightarrow b\bar{b}$

- important to distinguish $b\bar{b}$ and $c\bar{c}$ backgrounds from new physics signals

- LHC essentially a gg collider

- bottom fraction of D^{*+} is produced predominantly by $b\bar{b}$ and will contribute heavily to backgrounds

- charm production dominates bottom production by factor of 15 and also contributes to backgrounds

- the bottom and charm production fractions will be used to tune Monte Carlo simulations

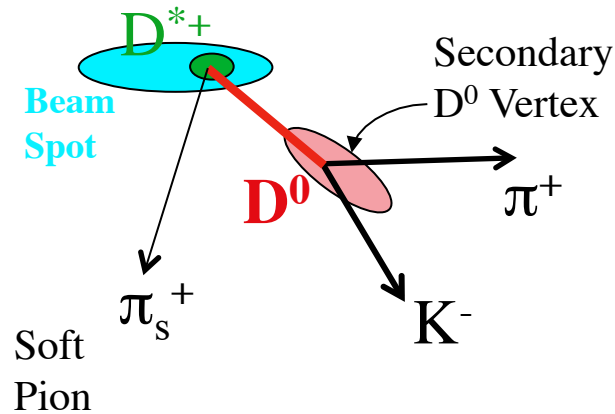
- b, c fractions provide insight into the parton distributions and production fractions



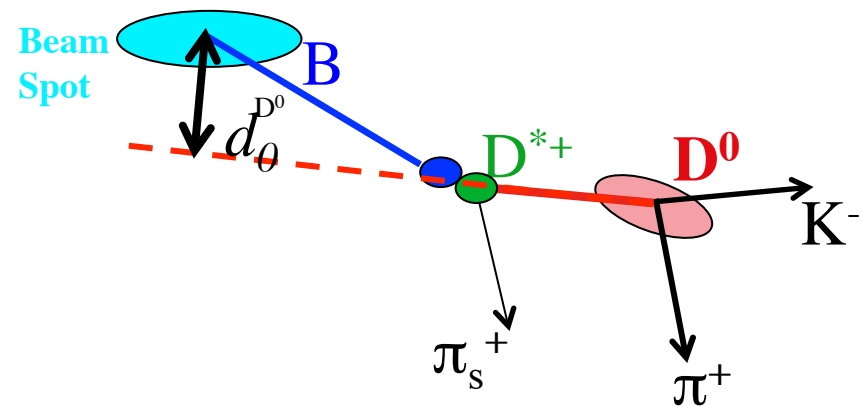
Strategy: Impact Parameter



Prompt Decay:



B Meson Decay:



Strategy:

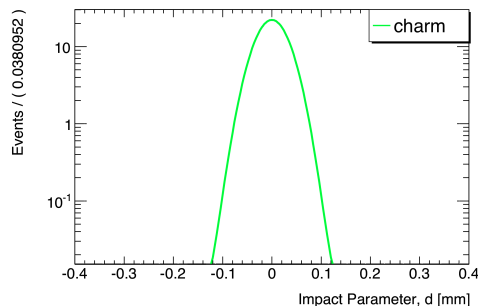
- The impact parameter of the D^0 , $d_0^{D^0}$, is used to distinguish the contributions from charm and bottom particles
- D^{*+} decays via strong interaction directly at production vertex or from a B meson decay



Strategy: Impact Parameter

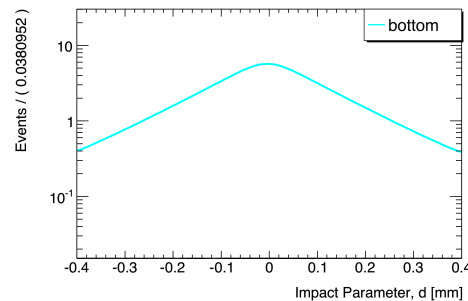


Prompt Decay:



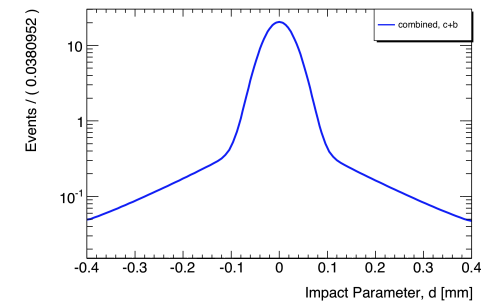
+

B Meson Decay:



=

Combined:



Strategy:

- The impact parameter distribution is modeled by:

$$F(d_0) = (1 - f_c)F_b \otimes F_D + f_c F_D$$

- F_b is the ideal (generator level) impact parameter distribution determined from MC
- F_D is the detector resolution modeled from prompt MC data
- The distributions of F_b and F_D are fixed and the charm fraction, f_c , is extracted from a fit to the D^0 meson impact parameter, d_0 , signal data



Data Selection



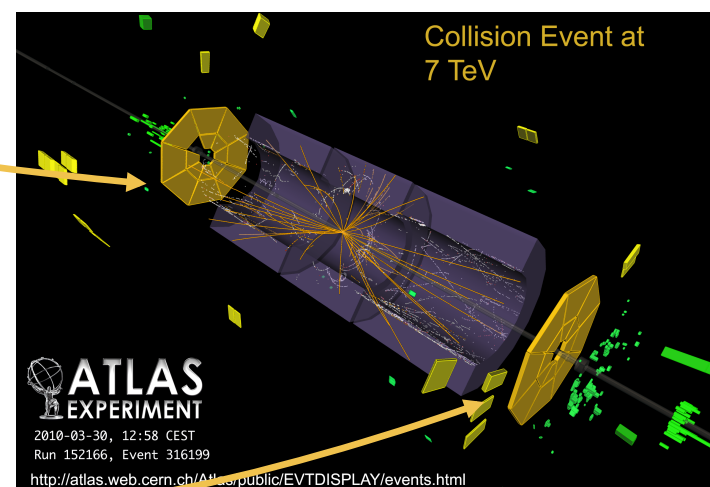
Minimum Bias Data:

- Minimum Bias Scintillator hit
- 2010 7 TeV data
- D^{*+} tracks:
 - 1 Pixel hit
 - 4 SCT hits
 - $p_T(K, \pi) > 1 \text{ GeV}$
 - $p_T(\pi_s) > 0.25 \text{ GeV}$

Monte Carlo:

- enriched with D meson decays
- 7 TeV PythiaB

Minimum Bias Scintillator

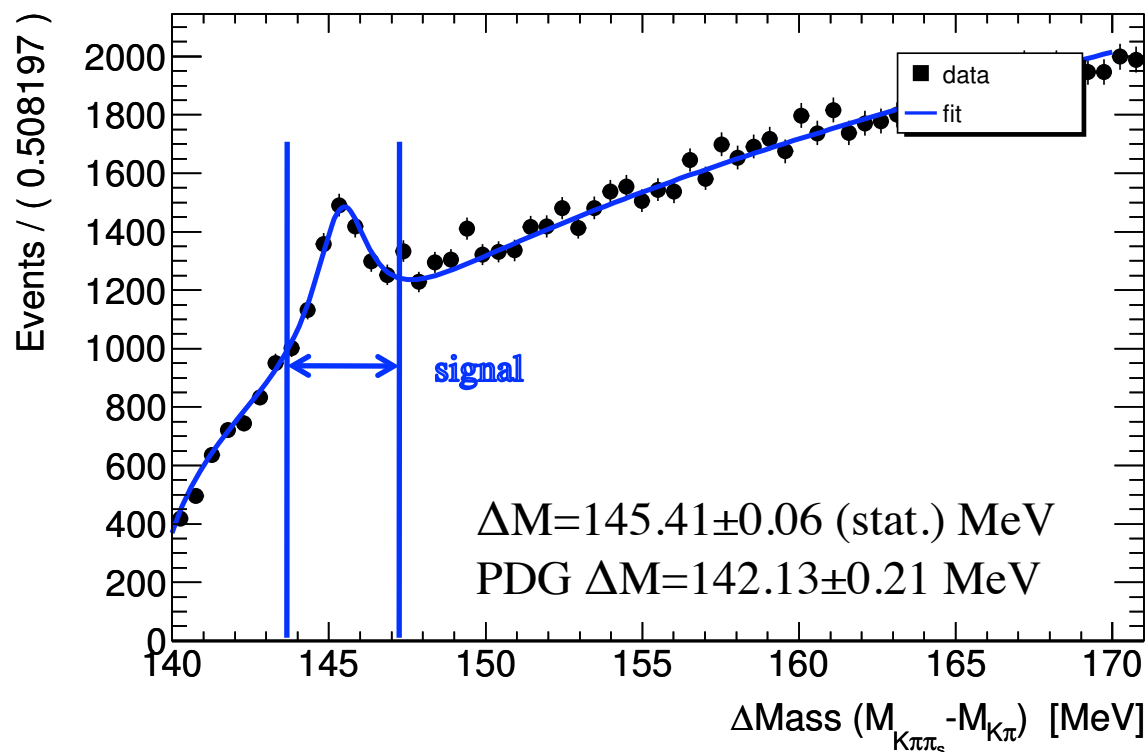




$\Delta\text{Mass} (M_{K\pi\pi} - M_{K\pi})$



MinBias Data



- Reconstruct D^{*+} event
- Fit $\Delta\text{Mass}(M_{K\pi\pi} - M_{K\pi})$
- Signal — Modified Gaussian:

$$f(x) = e^{-0.5x(1 + \frac{1}{1+0.5x})} \quad x = \left| \frac{\Delta M - \Delta M_0}{\sigma} \right|$$
- Background — Threshold Function:

$$f(\Delta M) = A \cdot (\Delta M - 0.13957)^B \cdot e^{C \cdot (\Delta M - 0.13957)}$$
- Select *signal* within 2σ of mean
 - $\sigma = 0.79 \pm 0.05 \text{ MeV}$



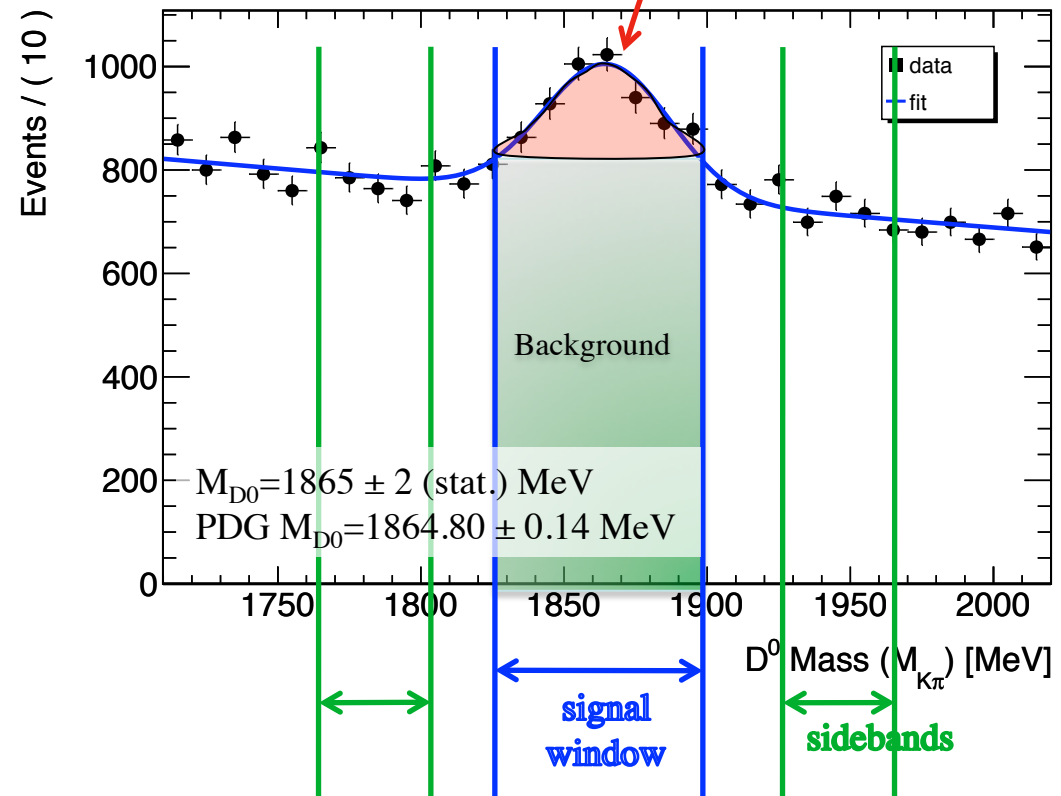
D⁰ Signal Selection



- Fit D⁰ mass of selected Δ Mass data
 - MC: modified gauss + exponential
 - MB: gauss + chebychev
- Select signal data within 2σ of mass peak
 - $\sigma = 22 \pm 2$ MeV
- Select sideband within 3-5 σ

=> For the corresponding D⁰ impact parameter data, subtract weighted sidebands from the signal region for the final signal data used in charm fraction fit

MinBias 7 TeV Data:



Select Signal = Signal Window – Background
Background = weighted sidebands



Detector Resolution, F_D



Detector resolution, F_D :

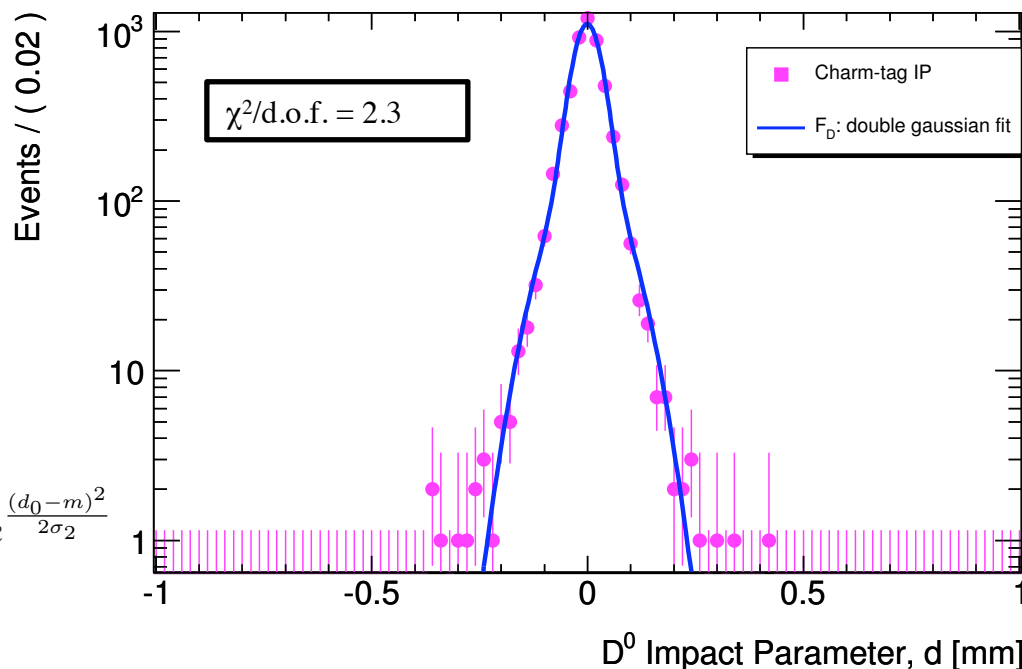
- Data: prompt tagged MC signal
- Choice of fit optimized from gaussian, double gaussian, gaussian + exponential, modified gaussian, gaussian + modified gaussian
- Selected double gaussian fit:

$$F_D(d_0) = f_1 \frac{1}{\sqrt{2\pi}\sigma_1} e^{-\frac{(d_0-m)^2}{2\sigma_1^2}} + (1 - f_1) \frac{1}{\sqrt{2\pi}\sigma_2} e^{-\frac{(d_0-m)^2}{2\sigma_2^2}}$$

- Extracted fit variables:

- $m = 0.0009 \pm 0.0006$ mm
- $\sigma_1 = 0.068 \pm 0.003$ mm
- $\sigma_2 = 0.028 \pm 0.0012$ mm
- $f_1 = 0.32 \pm 0.04$

April 25th, 2012



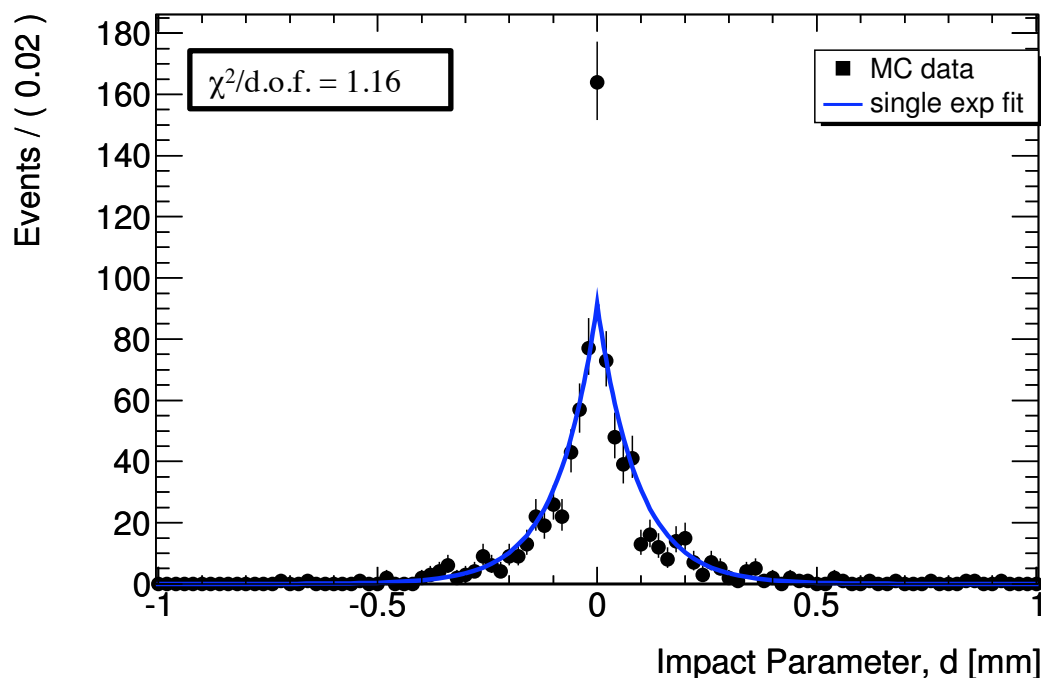


Ideal $b \rightarrow D^{*+}$



D^0 impact parameter distribution for *ideal* (generator level MC) $b \rightarrow D^{*+}(D^0\pi_s)$ events

- Modeled by: $F_b = \frac{1}{2\lambda_1} e^{-\frac{|d_0|}{\lambda_1}}$
- selected from single and double exponential functions



Extracted fit variable:
 $\lambda_1 = 0.092 \pm 0.003$ mm



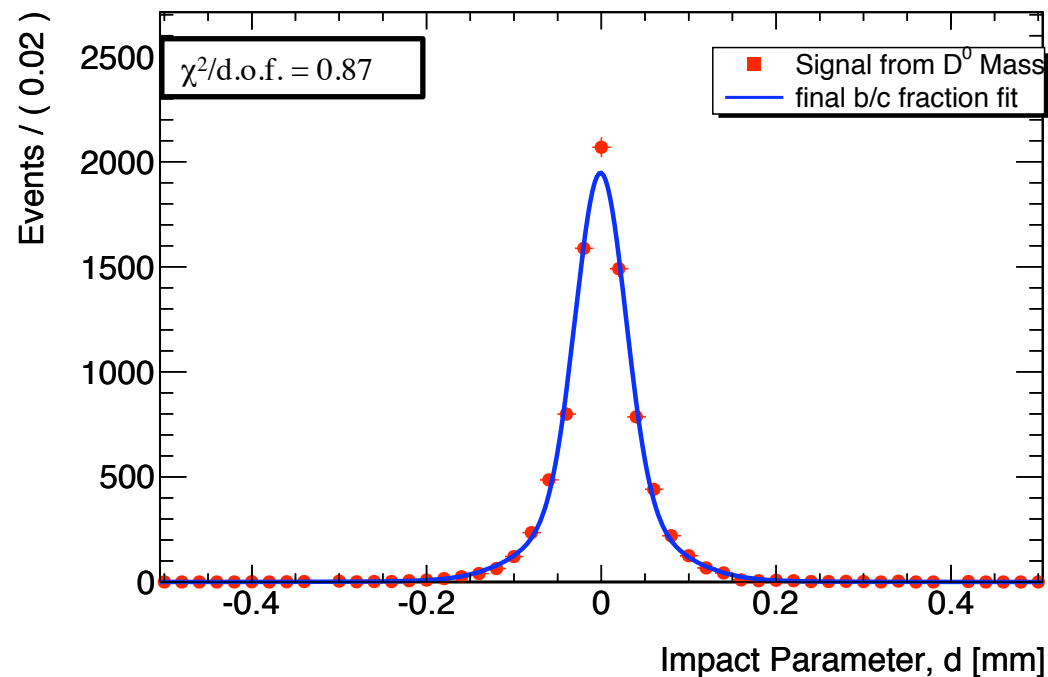
Charm Fraction Fit on Monte Carlo



Charm fraction fit on MC:

- $f_c = 97\% \pm 21\%$ (stat.)
- true $f_c = 96.4\%$

$$F(d_0) = (1 - f_c)F_b \otimes F_D + f_c F_D$$

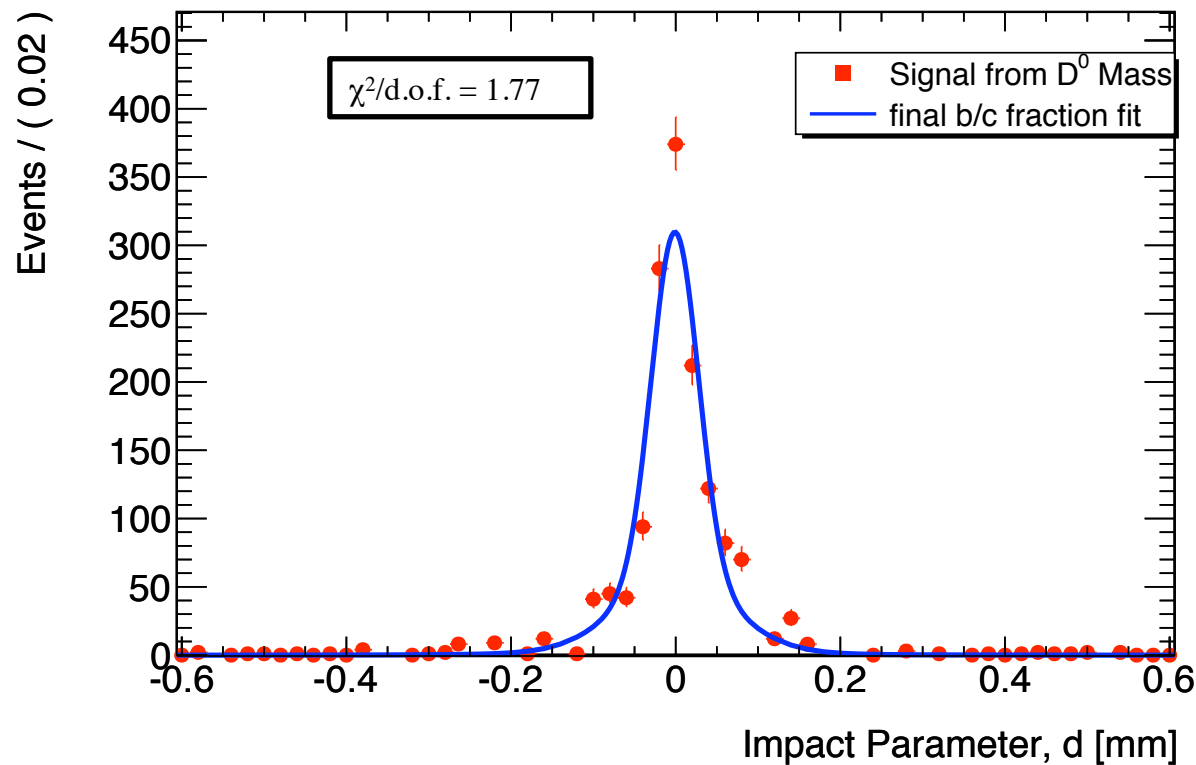




D⁰ Impact Parameter



Final fit to extract charm fraction, f_c , from D⁰ impact parameter signal



$$f_c = 96\% \pm 18\% \text{ (stat.)} \pm 0.8\% \text{ (sys.)}$$



b/c fractions Summary



- Developed procedure to measure charm fraction of $D^{*+} \rightarrow D^0(K^-\pi^+)\pi_s^+$ (+ c.c.)

- Model the impact parameter by:

$$F(d_0) = (1 - f_c)F_b \otimes F_D + f_c F_D$$

$$F_D(d_0) = f_1 \frac{1}{\sqrt{2\pi}\sigma_1} e^{-\frac{(d_0-m)^2}{2\sigma_1^2}} + (1 - f_1) \frac{1}{\sqrt{2\pi}\sigma_2} e^{-\frac{(d_0-m)^2}{2\sigma_2^2}}$$

$$F_b = \frac{1}{2\lambda_1} e^{-\frac{|d_0|}{\lambda_1}}$$

- Promising initial results

- MC Data: found $97\% \pm 21\%$ charm fraction, 96.4% from truth

- MinBias Data: $96\% \pm 18\%$ (stat.) $\pm 0.8\%$ (sys.) charm fraction

- Knowledge of bottom production in ATLAS is essential for background studies of flagship searches such as top and Higgs production, for example $H \rightarrow b\bar{b}$, since the b fraction of D^{*+} is generated primarily by $b\bar{b}$

Talk: A Measurement of the b and c Production Fractions with Fully Reconstructed D^{*+} Mesons in the ATLAS Detector at $\sqrt{s}=7$ TeV; Talk at the American Physical Society April Meeting 2011, Anaheim, CA, USA.



Review



Wide variety of contributions to ATLAS

- Commissioning
 - HVPP4
- ATLAS Upgrade
 - Planar materials (n- & p-type Fz & MCz)
 - irradiation and annealing effects on depletion voltage
 - defect behavior in mixed irradiations (not presented)
 - 3D sensors
 - capacitance measurements for a range of fluences
 - SiGe HBT electronics
 - irradiation effects on gain measurements
- Bottom and Charm Physics
 - measurement of b/c fractions to D^{*+} channel



Future Plans



Short Term: Postdoc

- split my time between hardware and physics analysis
 - Hardware: detector development
 - Physics Analysis: open to new topics, join ANL effort that needs manpower

Long Term:

- detector expert at a national laboratory



Back-up



Back-up



Planar Sensors



n-type MCz sensors

Mixed Irradiations: neutron & gamma

- Neutrons: 0.8-1 MeV (Hardness Factor=1.3), $1.5-3 \times 10^{14}$ n_{eq}/cm^2 , Annular Core Research Reactor in Sandia National Lab
- Gamma: 1.25 MeV ^{60}Co , BNL, up to 500 Mrads

Experimental Technique:

- low temp IV, CV (at UNM)
- IV, CV, and TCT [2] with red (660 nm) laser (measured at BNL)

Sample #:	1480-5	1480-13	1480-15	1480-16
Conditions:				
1 st Radiation: Neutron (n_{eq}/cm^2)	1.5×10^{14}	1.5×10^{14}	3×10^{14}	3×10^{14}
2 nd Radiation: Gamma (Mrad)	500	0	0	500



Planar Sensors

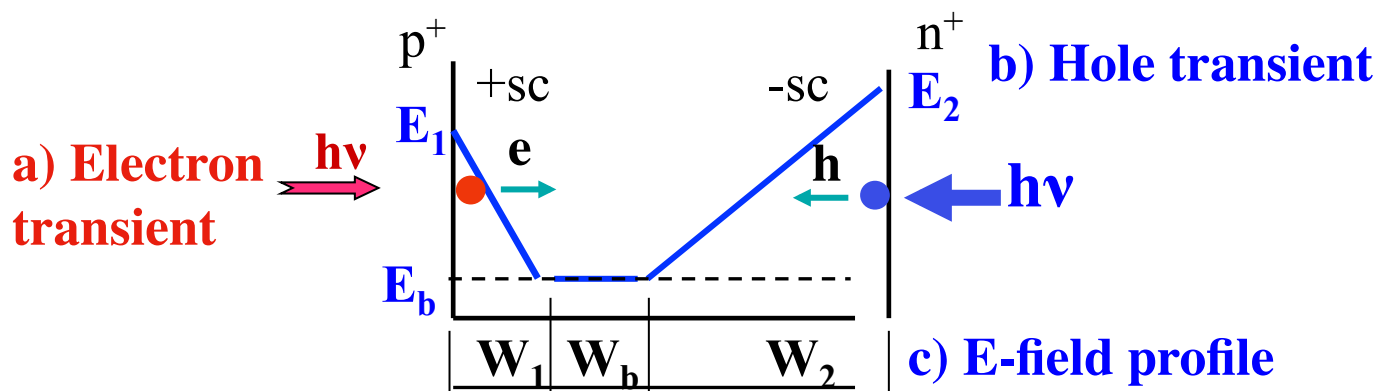
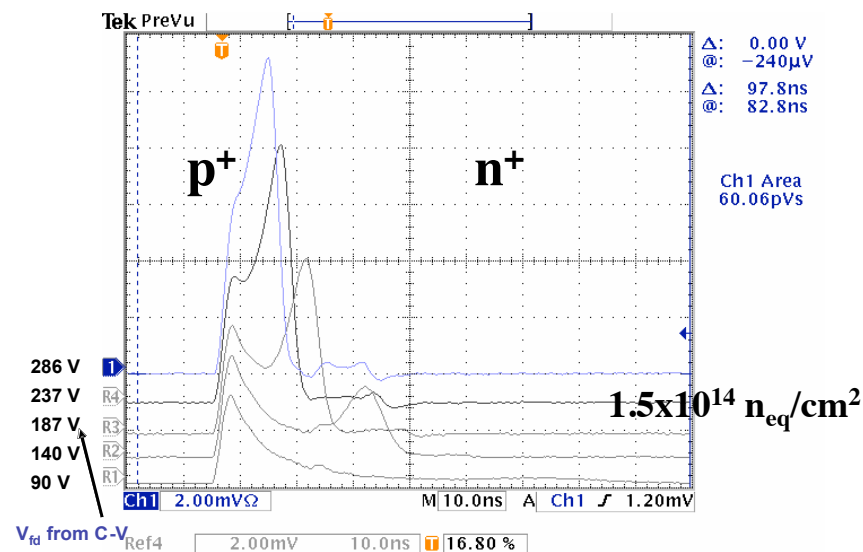


1480-13, $1.5 \times 10^{14} \text{ n/cm}^2$ (22 d RT anneal), MCZ n-type Si, p⁺/n/n⁺ structure

Laser front, electron current from p⁺ to n⁺
Double junction, and SCSI seen

TCT Measurement:

- pulse laser on front or back
 - determines collection of electrons or holes
- shape of signal depends on electric field profile
- Electron Current:
 - +sc = decreasing current
 - -sc = increasing current





Planar Sensors



Temperature Effects:

- observation of low temperature leakage current suppression
- decrease in V_{fd}

	Full Depletion Voltage:	
Measurement Location:	UNM	BNL
Temperature:	$\sim -10^\circ\text{C}$	$+20^\circ\text{C}$
Sample #:		
1480-5 (1.5×10^{14} n/cm ²)	<10	276
1480-13 (1.5×10^{14} n/cm ²)	13	275
1480-14 (3×10^{14} n/cm ²)	20	-
1480-16 (3×10^{14} n/cm ²)	13	782

- neutron irradiations include 22 days RT anneal time
- reverse annealing done for 5.5 months at RT
- reverse annealing suppressed in gamma irradiated samples
- +sc introduced by gamma irradiation should compensate for -sc introduced by neutron irradiation in 1.5×10^{14} n/cm², but not enough in 3×10^{14} n/cm²
→ interaction of defects

Mixed Irradiation Effects:

Sample #	Neutron Irradiation: V_{fd} [V]	N_{eff} [cm ³]	Reverse Annealing: V_{fd} [V]	N_{eff} [cm ³]
1480-13 1.5×10^{14} n/cm ² No Gamma	187	-1.5×10^{12}	400	-3.3×10^{12}
1480-14 3×10^{14} n/cm ² No Gamma	507	-4.2×10^{12}	≥ 1100	$\leq 8.9 \times 10^{12}$
1480-5 1.5×10^{14} n/cm ² 500 Mrad	177	-1.5×10^{12}	170	-1.4×10^{12}
1480-16 3×10^{14} n/cm ² 500 Mrad	508	-4.2×10^{12}	508	-4.2×10^{12}



Planar Sensors



Summary of Mixed Irradiations Study:

- Space Charge Sign Inversion (SCSI) was confirmed for n-type MCz
- Gamma irradiation after neutron irradiation suppresses long-term (“reverse”) annealing effects
 - independent of neutron fluence
 - points to interaction of gamma induced defects during long-term annealing process
- New understanding of the behavior of silicon in response to radiation increases the potential of designing better detectors for high luminosity applications

Publication: Observations of Gamma Irradiation-Induced Suppression of Reverse Annealing in Neutron Irradiated MCZ Si Detectors: Zheng Li, Rubi Gul, Jaakko Harkonen, Jim Kierstead, J. Metcalfe, Sally Seidel. IEEE Nuclear Science Symposium Conference Record, pp1597-1599, October 2008.

Talk: June 2008 RD50 Workshop, Ljubljana, Slovenia



Systematic Errors



Systematic error analysis:

- choice of fit
- choice of bin size
- selection range
- F_b and F_D statistical errors propagated to f_c

ATLAS error sources absorbed by MC studies:

ATLAS Error Source	Error
primary vertex	$10 \mu\text{m}$
track d_0	$22 \mu\text{m}$
σ/p_T	$3.8 \times 10^{-4} p_T \text{ GeV} \pm 0.015 \text{ GeV}$

Propagate statistical errors to f_c :

Fit Parameter	f_c Error
$F_b: \lambda - 1\sigma$	0.087%
$F_b: \lambda + 1\sigma$	0.083%
$F_D: m - 1\sigma$	0.03%
$F_D: m + 1\sigma$	0.03%
$F_D: \sigma_1 - 1\sigma$	0.108%
$F_D: \sigma_1 + 1\sigma$	0.059%
$F_D: \sigma_2 - 1\sigma$	0.103%
$F_D: \sigma_2 + 1\sigma$	0.088%
$F_D: f_1 - 1\sigma$	0.17%
$F_D: f_1 + 1\sigma$	0.112%
Total Systematic Error:	0.3%

Table 5.10: Charm Fraction Fit Systematic Errors

Error Source	f_c Error
Choice of F_D Fit	1.4%
Choice of F_b Fit	0.5%
F_D Bin Size	1%
F_b Bin Size	0.0%
Choice of Signal Selection Range	0.5%
Statistical Errors Propagated to f_c	0.3%
Total Systematic Error:	0.8%



Back-up



Inner Detector Tracking Efficiency

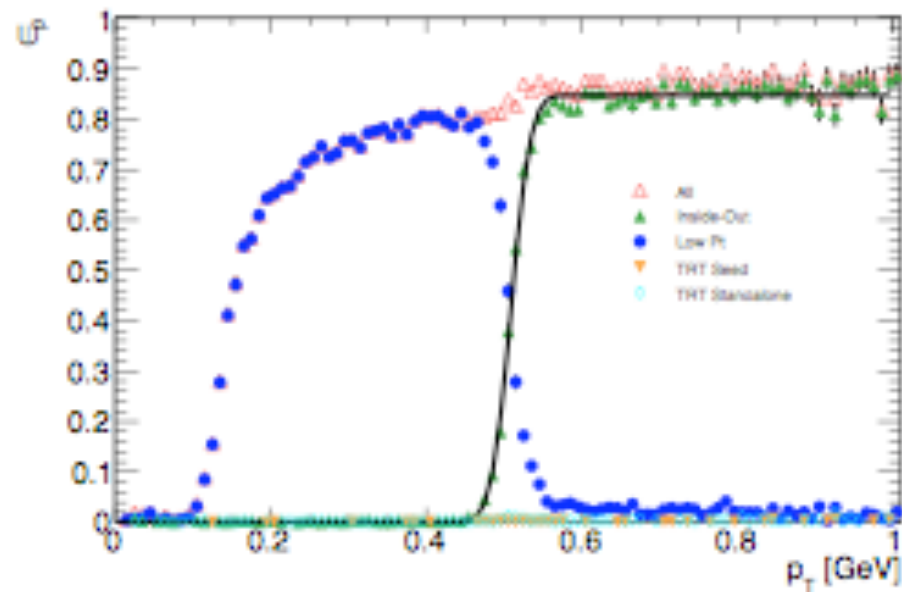
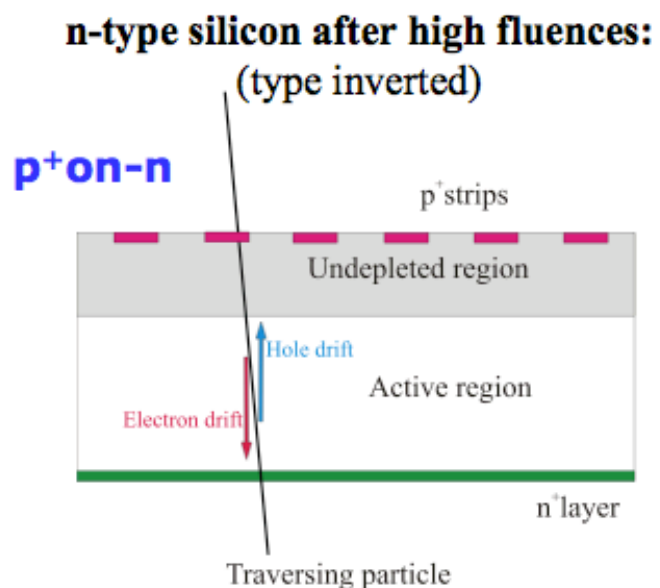


Figure 2: The tracking efficiency as a function of track p_T for the different tracking algorithms.

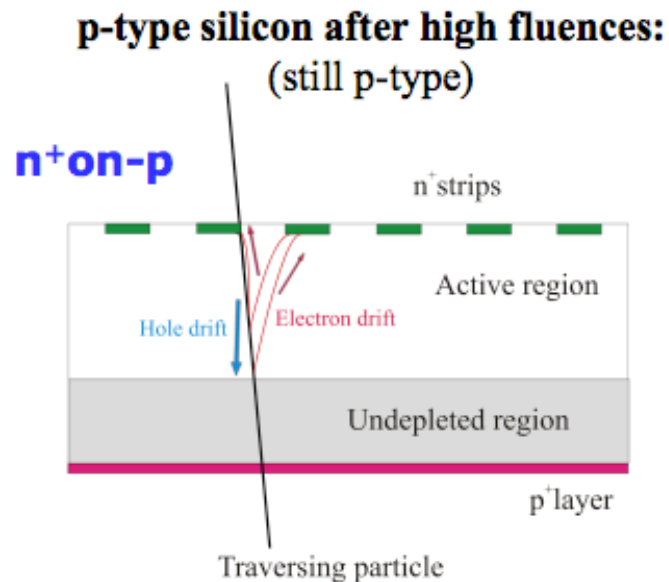


Back-up



p-on-n silicon, under-depleted:

- Charge spread – degraded resolution
- Charge loss – reduced CCE



n-on-p silicon, under-depleted:

- Limited loss in CCE
- Less degradation with under-depletion
- Collect electrons (3 x faster than holes)

Comments:

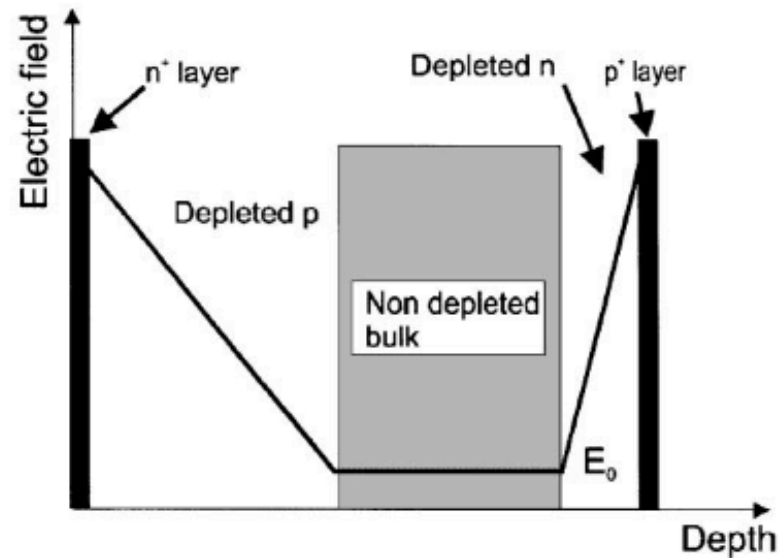
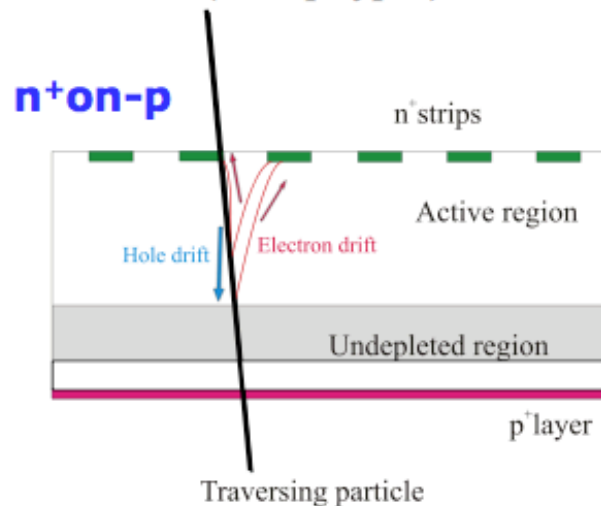
- Instead of n-on-p also n-on-n devices could be used



Back-up



p-type silicon after high fluences:
(still “p-type”)



- **Dominant junction close to n⁺ readout strip for FZ n-in-p**
- **For MCZ p-in-n even more complex fields have been reported:**
 - no “type inversion”(SCSI) = dominant field remains at p implant
 - “equal double junctions” with almost symmetrical fields on both sides

Michael Moll – Instrumentation Seminar, Hamburg 26.3.2010 -33-



Introduction to ATLAS



- The Inner Detector tracks charged particles that traverse the detector
- Beam
 - 30 μm transverse length, 5.6 cm (1σ) in z
- In a 2 Tesla field
- p_T threshold: 500 MeV (100 MeV low p_T)
- Pixel
 - resolution: 10 μm in $R-\Phi$, 115 μm in z
- SCT (Semi-Conductor Tracker)
 - resolution: 17 μm in $R-\Phi$, 580 μm in z
- TRT (Transition Radiation Tracker)
 - overall resolution: 130 μm

